Chemical Engineering & Processing: Process Intensification 218 (2025) 110559

Contents lists available at ScienceDirect

Chemical Engineering and Processing - Process Intensification

journal homepage: www.elsevier.com/locate/cep

Beyond dividing wall columns: Improved process intensification through liquid-only transfer and heat integration

Momme Adami [a], Sina Bertram [a], Dennis Espert [a], Mirko Skiborowski [a,b,*]

[a] Hamburg University of Technology, Institute of Process Systems Engineering, Am Schwarzenberg-Campus 4, 21073 Hamburg, Germany
[b] United Nations University Hub on Engineering to Face Climate Change at the Hamburg University of Technology, United Nations University Institute for Water, Environment and Health (UNU-INWEH), Hamburg, Germany

ARTICLE INFO

Keywords:
Distillation
Dividing wall column
Heat integration
Liquid only transfer
Shortcut screening
Superstructure optimization

ABSTRACT

Many chemical companies aim to achieve climate neutrality by 2050, requiring raw material changes and significant reductions in process energy. Since distillation accounts for a large share of energy use, it is a key target for process improvements. One promising approach is thermal coupling between columns, which is already industrially implemented, especially in dividing wall columns. However, such configurations often suffer from limited operational flexibility due to the fixed vapor split between parallel sections, which is largely fixed during design and difficult to adjust during operation. This limitation can be overcome by replacing each bidirectional vapor-and-liquid connection with a liquid-only transfer side stream. This concept allows each column to operate at an individual pressure and enables new options for heat integration. The present study introduces a structured approach for assessing and optimizing such systems with one or two liquid-only transfer side streams, particularly when combined with direct heat integration. Promising configurations are first identified through an efficient shortcut screening and can further be optimized using superstructure optimization. A case study on separating benzene, toluene, and para-xylene demonstrates that liquid-only transfer configurations with direct heat integration can significantly reduce energy and costs, and in many cases outperform conventional thermally coupled systems.

1. Introduction

In order to mitigate the consequences of climate change, there is a great need to reduce the energy demand and greenhouse gas emissions. This reduction is essential not only for environmental protection but also for the economic viability of energy-intensive sectors including the chemical industry, which ranges among the largest consumers of energy worldwide [1]. For instance, projections indicate that within the next two decades, carbon prices in the European emissions trading system could reach several hundred euros per ton of CO_2-equivalent [2] shown in Fig. 1. Consequently, reducing emissions will be vital for ensuring economic competitiveness in the coming decades, a trend already observed during periods of high energy prices in the past when the adoption of energy-efficient technologies surged.

In the chemical industry, thermal separation processes account for the majority of the process energy [3], with distillation processes as the most dominant technology, accounting for more than 90 % of industrial fluid separations [4]. Due to the extensive use of distillation and the significant contribution to the industrial energy demand, process intensification strategies have gained significant attention. Especially, since other unit operations are not inherently more efficient than distillation [5,6] simple substitution is in most cases not feasible. Different energy integration methods have been established [7] to improve the energy efficiency of distillation processes, which can also achieved by hybridization with other separation technologies such as extraction, membrane separations and hybrid separation processes [8, 9].

For simple distillation columns heat pump assisted distillation may be applied based on different concepts [10], all of which are based on the recovery of rejected heat by raising its temperature using compressors, offering both energy and emission reductions. Mechanical vapor recompression (VRC) is most commonly applied [11]. Especially flash-enhanced VRC configurations can enable full electrification of the process with net energy savings reported of over 95 %, closely matched by closed-cycle heat pumps with properly selectable refrigerants [12]. Further intensification in terms of internally heat-integrated distillation columns (HIDiC) have been rarely applied in industrial settings [13].

* Corresponding author.
E-mail address: mirko.skiborowski@tuhh.de (M. Skiborowski).

https://doi.org/10.1016/j.cep.2025.110559
Received 26 July 2025; Received in revised form 8 September 2025; Accepted 17 September 2025
Available online 18 September 2025

Nomenclature

b	Binary decision variable
$\dot{B}$	Molar flow rate of bottom stream
c	Column index
D	Column diameter
$\dot{D}$	Molar flow rate of distillate stream
DIPPR	Design Institute for Physical Properties
DLL	Dynamic link library
DWC	Dividing wall column
e(z)	External equations
f	Feed
F	F-Factor
$\dot{F}$	Molar flow rate of feed
PF-FC	Prefractionator with full thermal coupling
GAMS	General Algebraic Modeling System
h	Specific enthalpy
h^L	Specific liquid enthalpy
h^V	Specific vapor enthalpy
HI	Direct heat integration
HI12	Direct heat integration from column 1 to column 2
HI21	Direct heat integration from column 2 to column 1
HI-XYZ-MP (e.g. HI-123-MP)	Middle pressure, Heat integration from column X (high pressure) to column Y (base pressure), and from column Y to column Z (low pressure)
HIDiC	Internally heat-integrated distillation column
HP	High pressure, Heat integration by pressure increase
i	Product fraction
$\dot{K}$	Molar flow rate of boil-up stream
LOT	Liquid only transfer
LP	Low pressure, Heat integration by pressure decrease
$\dot{L}$	Molar flow rate of liquid stream
m	non-divided sections of dividing wall column
MED	Minimum energy demand
MES	Material, equilibrium, summation
MESH	Material, equilibrium, summation, enthalpy
MINLP	Mixed-integer nonlinear programming
$\dot{n}$	Flowrate
n	Stage number
n_{max}	Maximum number of equilibrium stages
NLP	Nonlinear programming
NRTL	Non-Random Two-Liquid
PF-PCC	Prefractionator with partial thermal coupling at the condenser
PF-PCR	Prefractionator with partial thermal coupling at the reboiler
PF	Prefractionator
$\dot{Q}$	Heating / cooling duty
$\dot{R}$	Molar flow rate of reflux stream
s	Side stream
$\dot{S}$	Molar flow rate of side stream
SLOPPY	Sloppy split configuration
SNOPT	Sparse nonlinear optimizer
SR	Side rectifier
SS	Side stripper
TAC	Total annualized cost
$\dot{V}$	Molar flow rate of vapor stream
V_{min}	Minimum vapor flow
VRC	Mechanical vapor recompression
x	Composition of liquid phase
y	Composition of vapor phase
z	Total composition; set of variables transferred from GAMS
ψ	Distribution factor

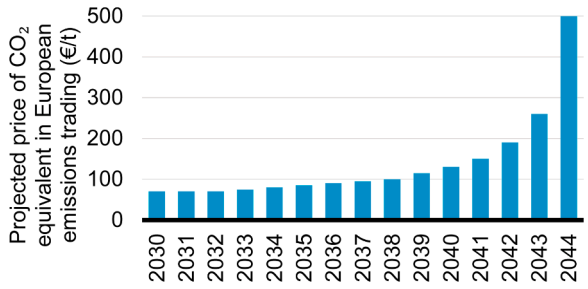

Fig. 1. Projected price of CO2 equivalent in European emissions trading between 2030–2044 [2].

Despite the possible approximation of a reversible distillation by a continuous heat transfer in diabatic column sections, the adjustment to the internal temperature profiles presents a significant challenge [14], and techno-economic optimization studies have found VRC designs to be at least competitive and oftentimes superior [15,16].

Another means for energy savings for simple distillation columns is multi-effect distillation, for which the feed stream can be divided among multiple heat integrated columns operating at different pressures [17]. Alternatively, the feed is processed in a sequence of columns which consistently produce (almost) the same product, while the other product is progressively purified in the subsequent columns. Such configurations are common for seawater desalination [18] or methanol distillation [19]. Despite the possible high energy savings, both, multi-effect distillation and heat pump assisted distillation require significant capital investment for additional compressors or columns, respectively.

For separations involving three or more products, direct heat integration (HI) offers a capital-efficient approach by adjusting operating pressures to enable a sufficient temperature driving force between a top vapor stream of one column and the liquid bottoms stream of another column to be heat integrated. This may spare up to 50 % of the net energy requirements. Alternatively, thermal coupling can be used, where bidirectional liquid and vapor transfers replace conventional heat exchangers between adjacent columns [20] effectively combining heat and mass integration, reducing mixing losses. Thermal coupling itself and equipment integrated dividing wall columns (DWC) are considered as one of the most prominent examples of process intensification in fluid separations. Since the first reported industrial DWC at BASF in 1985 [21], DWCs have been widely adopted, with over 300 reported industrial implementations [22]. They reportedly possess the potential for energy and operating cost reductions of 30–40 % compared to non-integrated process configurations, combined with up to 30 % reduced investments for DWCs [23,24]. Existing units today have diameters of over 6 m and heights of over 100 m [25]. However, the optimal design and control of dividing wall columns (DWCs) can be a challenging task due to the large number of design decisions, including the vapor split, and the nonlinear behavior in operation [26].

While usually a choice has to be taken between either classical thermal coupling and HI since the vapor transfer between thermally coupled column sections impedes separate pressure variation, this limitation can be overcome by converting thermal coupling links to unidirectional liquid-only transfer (LOT) streams with extended column sections and individual heat exchangers [27]. These effectively enable independent control of vapor flow in each column, while preserving the energy benefits of thermal coupling [28]. Skiborowski [29] and Adami et al. [30] have illustrated by shortcut evaluations that LOT

modifications of side strippers and side rectifiers with direct HI provide the lowest energy demand for a wide range of feed compositions for the separation of some test systems, with energy savings of up to 30 % compared to the fully thermally coupled DWC.

The current work extends these investigations on LOT configurations by developing a systematic framework for their design, evaluation, and optimization, both with and without direct HI. Following the concept of the process synthesis framework [9,31], pinch-based shortcut evaluations are first employed to rapidly assess the potential net energy savings of these configurations for specific separation tasks in comparison with fully coupled DWCs and other heat-integrated sequences. In a subsequent step, the most promising options are further analyzed using rigorous techno-economic optimization based on equilibrium-stage superstructure models to validate the shortcut results and identify the best designs for LOT flowsheets benefitting from the combined effects of thermal coupling and HI. The performance of these configurations is evaluated in terms of energy savings and economic improvements.

After providing a more detailed analysis of thermally coupled processes in Section 2, as well as the required modifications to LOT sidestream configurations in Section 3, the design method is presented in Section 4. First, the utilized shortcut screening is summarized in Section 4.1, followed by a detailed description of the optimization models and solution strategy for the techno-economical optimization in Section 4.2. Section 5 illustrates the application of the method for the separation of a benzene, toluene, and p-xylene mixture. Finally, Section 6 provides a conclusion and an outlook on future work.

2. Revisiting thermal coupling

In a conventional distillation sequence, each column requires a minimum heat duty to provide the minimum vapor flow that is necessary to perform the more complex separation, either in the rectifying or stripping section. The net energy requirement of the sequence is determined as the sum of the minimum heat duties of the individual columns. In a thermally coupled configuration, however, the columns in the sequence are connected by means of bidirectional vapor and liquid transfer, such that the individual vapor loads can be provided by splitting the total vapor load produced in a single reboiler of the thermally coupled configuration. In case of a fully thermally coupled, so-called Petlyuk configuration, the required minimum vapor load matches exactly that of the most complex separation in a simple column, which can be illustrated by means of the V_{min} diagram, introduced by Halvorsen and Skogestad [32–34]. Thermal coupling generally reduces energy demand as it avoids unnecessary heat demands for each individual separation by reducing mixing losses [35]. Nevertheless, the reduced heat demand also comes with a downside, as the required heat duties of thermally coupled generally need to be provided and removed at the more extreme temperature levels. Thus, despite the general reduction of the total net energy demand, thermally coupled configurations do not necessarily have higher exergetic efficiency [20].

Two structural types of thermal coupling can be distinguished:

1. In the first type, a heat exchanger which produces an intermediate product for a downstream column is replaced by bidirectional vapor-liquid transfer between the two columns. Because the columns normally appear side-by-side in a flowsheet, this is further referred to as *horizontal* thermal coupling.
2. The second type can be derived from two columns, which share the same product at their opposite ends. If both the condenser and the reboiler associated with this shared product have about the same absolute net heat duty, they can be substituted by bidirectional vapor-liquid transfer and the columns stacked in one shell such that the common product is withdrawn as a side stream, replacing two heat exchangers simultaneously. Due to the top-to-bottom interconnection, this is further referred to as *vertical* thermal coupling.

When horizontally coupling the connection between the columns in a direct sequence, as illustrated in Fig. 2, the column sections of the resulting thermally coupled direct sequence can be rearranged to the well-known side rectifier (SR) configuration. For further capital cost savings and process intensification the SR can also be implemented in an equipment-integrated split shell column with a dividing wall at the top, further referred to as a top-DWC. Importantly, the thermally coupled direct sequence, the SR and the top-DWC are all thermodynamically equivalent, meaning that they produce the same product streams at identical temperature levels while requiring the same amounts of heating and cooling. Thermodynamic equivalence can generally be understood as physically different implementations of the same conceptual model based on material and enthalpy balances, summation constraints and equilibrium models (MESH models).

Similar to the direct sequence, also the column sections of a thermally coupled indirect sequence can be rearranged to obtain a side stripper (SS) configuration, which again can be implemented in form of a split shell column with a dividing wall at the bottom, further referred to as bottom-DWC, as shown in Fig. 2. While the SR and its thermodynamically equivalent variants require a vapor split, the SS and its equivalent variants, only need a simpler to control liquid split.

In a sloppy split configuration, for which the first column, the so-called prefractionator, produces two intermediate products which separate the light and heavy boiling components, while distributing some intermediate boilers, the subsequent two columns purify the low and heavy boiling fractions, while producing the intermediate boilers the opposing ends. For this configuration both subsequent columns can be vertically thermally coupled at the opposing ends by replacing the individual heat exchangers with a bidirectional vapor and liquid transfer, merging the two columns into a single side stream column, as illustrated in Fig. 3. This configuration with the prefractionator column and the subsequent main column with two feed streams and a side stream is further referred to as basic prefractionator (PF) configuration.

In the PF both columns can further be thermally coupled by replacing the connecting streams and the heat exchangers for the prefractionator column by means of bidirectional vapor and liquid transfer, as illustrated in Fig. 4. If only one of the connections is transformed, the resulting configuration is considered to be a partially thermally coupled variants of the PF, either resulting in the PF with partial thermal coupling at the condenser (PCC) or partial thermal coupling at the reboiler (PCR). The PCC again avoids the need for a vapor split, since only liquid needs to be distributed. In case both connections are replaced by vapor-liquid transfer, a fully thermally coupled prefractionator (PF-FC) also known as the Petlyuk configuration is generated, which can be implemented as well-known dividing wall column with a central dividing wall (middle-DWC).

While thermal coupling generally reduces the net energy requirements and especially in the implementation of DWC provides additional investment cost savings, both oftentimes reaching up to 30 % [23,24], in the heat and mass integration comes with certain limitations for process design and operation. When replacing a connecting stream and a reboiler with a horizontally coupled vapor liquid transfer, this always results in a vapor split. Although, some concepts for active vapor split control have been proposed in literature [36–38], in practice it is usually not part of the control structure [39]. Instead, the vapor split is fixed during the design phase, reducing process flexibility during operation as only the liquid split can be adjusted during operation of DWC or other thermally coupled sequences [40].

Due to these challenges, the design [24,41–43] and operation [22, 44,45] of dividing wall columns has been covered extensively and both optimal design and effective control of middle-DWCs have proven possible. Current research focuses therefore on more complex configurations, such as the extension with multiple dividing walls for production of four product streams [24,46–49]. Despite these advancements, especially the vapor split may easily end up outside the optimal range during operation due to disturbances, making it difficult to achieve the

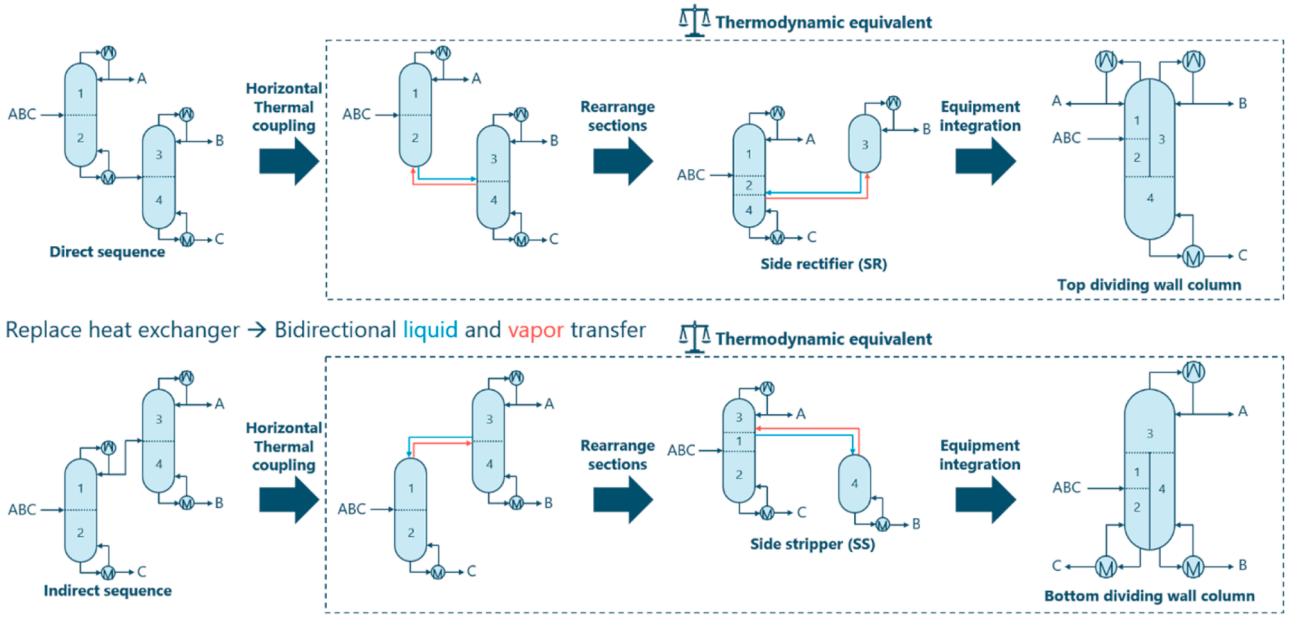

Fig. 2. Transition from direct (indirect) sequence to side rectifier (stripper) and its thermodynamically equivalent configurations via horizontal thermal coupling.

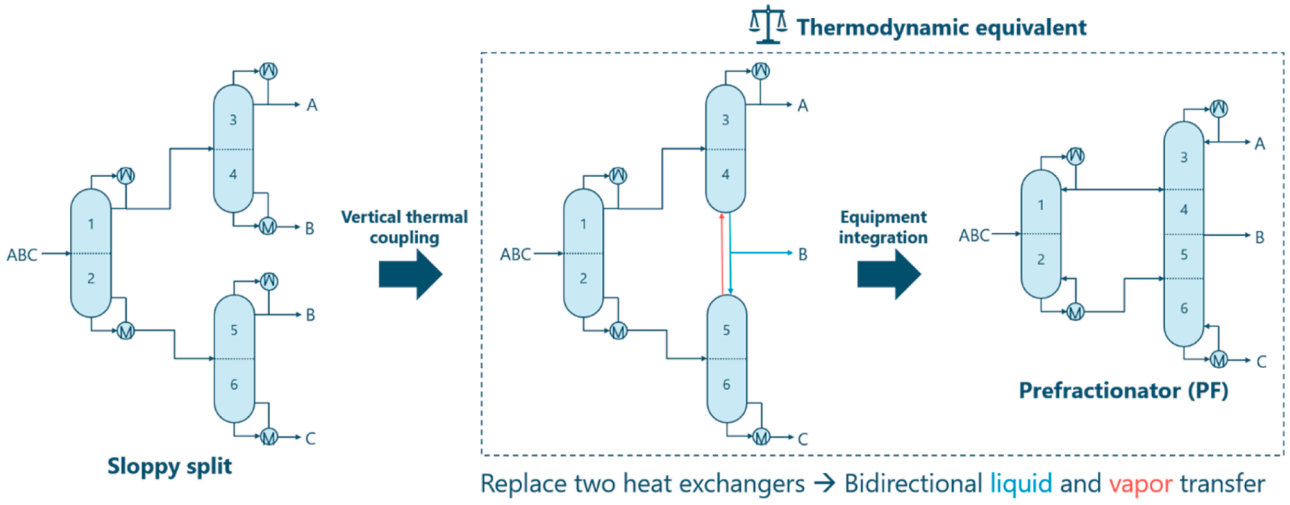

Fig. 3. Transition from sloppy split via vertical thermal coupling to prefractionator configuration.

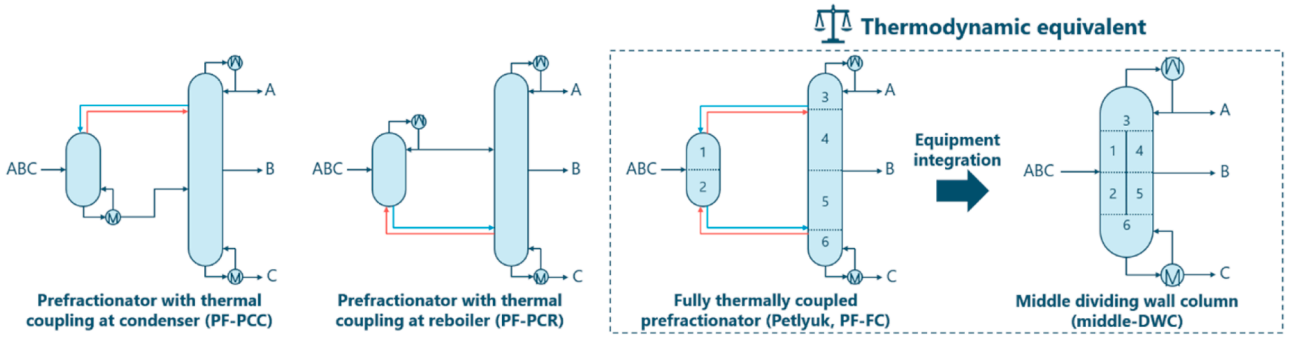

Fig. 4. Partially and fully thermally coupled variants of prefractionator configuration. The Petlyuk configuration can be equipment-integrated as a middle dividing wall column.

desired separation at minimum energy demand [40]. The vapor transfer furthermore results in a hydrodynamic link between the thermally coupled columns that impedes an individual pressure for the operation of the columns, preventing further heat integration. Therefore, based on the excellent work of Agrawal [27,50], alternative configurations have been proposed that retain the energy-saving benefits of thermal coupling while mitigating the operational challenges associated with vapor transfer.

3. Liquid only transfer: thermal coupling without vapor transfer via side streams

In order to overcome some of these limitations, horizontal thermal coupling links can be modified by adding column sections and heat exchangers in such a way, that the bi-directional vapor and liquid exchange is replaced with a unidirectional liquid side stream [27]. The so-called concept of liquid only transfer (LOT) preserves the energy benefits of horizontal thermal coupling while providing three key advantages over conventional thermally coupled configurations and DWCs as outlined in the recent review by Horsch and Skiborowski [28]:

Because LOT sequences connect columns with a liquid stream, each column can be operated at an individual pressure, such that the boiling points of individual products can be shifted to adjust for temperature sensitivity or utility limits. Such pressure variations further enable HI between condenser and reboiler of adjacent columns by adjusting the temperature levels [51]. It is further expected that LOT configurations allow for more flexible and robust operation at the energy-optimal operating point, since the liquid side streams and the additional heat exchangers provide additional degrees of freedom for process control. Finally, the implementation of LOT couplings allows for the retrofit of existing sequences to be upgraded into coupled systems with relatively low capital expenditure, delivering operating cost savings without extensive column modifications, as investigated by Horsch et al. [52].

For further illustration, the development of a fully thermally coupled prefractionator with LOT via two liquid side streams starting from to a Petlyuk configuration is shown in Fig. 5. Column sections (3X and 6X) with additional heat exchangers are added to the prefractionator producing the same top and bottom product as the main column, while providing the vapor flowrate, which is otherwise transferred between the columns. Thus, the respective heat duties are distributed between the pre-existing and the newly added heat exchangers. Since additional heat exchangers and stages are required, LOT configurations generally have higher investment cost than their thermally coupled counterparts. The respective transformations for SS and SR are elaborated in the articles of Adami et al. [30] and Horsch and Skiborowski [28].

It is important to note that Ramapriya et al. [53] have provided a proof that LOT configurations can generally be designed thermodynamically equivalent to their thermally coupled counterparts. In addition, Halvorsen and Skogestad [54] have recently shown that a derived analytical minimum energy expression for the LOT arrangement is identical to that for the standard DWC.

Due to the hydrodynamically independent operation of the individual columns, LOT configurations provide further potential for HI. However, heat exchangers at intermediate temperature levels are removed in thermally coupled and LOT configurations, larger pressure modifications are required to obtain product temperatures suitable for the remaining HI possibilities.

4. Methods

For the evaluation and optimization of LOT processes without and with HI, we follow the concept of the process synthesis framework Marquardt et al. [55]. Therefore, a pre-defined selection of potential process configurations is evaluated by means of a pinch-based shortcut screening framework, as previously presented by Skiborowski [56] and further developed by Adami et al. [57,58], to rapidly compare the different configurations on the basis of minimum energy demand and total annual cost estimates. The current publication addresses specifically the potential of LOT configurations and therefore extended the framework by five LOT process variants with one and two side streams, for which furthermore 20 LOT configurations with additional HI are derived. Thus, in total 25 LOT configurations are evaluated in comparison to simple sequences, as well as thermally coupled and other energy-integrated distillation processes.

The most promising configurations identified during the shortcut screening are further analyzed using rigorous techno-economic optimization based on equilibrium-stage superstructure models, using a proven approach previously presented for individual columns [59] and energy integrated sequences including DWCs [24,43]. The results of these optimizations serve as validation of the shortcut screening and provide the basis for further investigations and detailed engineering studies. The results of the shortcut evaluations provide valuable information for the initialization of the rigorous models, enabling improved convergence.

4.1. Shortcut screening for minimum energy demand and cost estimates

The individual elements of the shortcut screening as introduced by [30,56,58] are illustrated in Fig. 6. The computations are based on a given specified feed composition and flow rate, along with the targeted product compositions and a baseline operating pressure, while the required thermodynamic property parameters can be transferred from Aspen properties. The MATLAB-based tool subsequently evaluates various process configurations, each considering a sequence of distillation columns with different means for heat and mass integration. For each alternative, a specified model of the process configuration is evaluated on the basis of minimum energy demand (MED) computations, building on the Rectification Body Method, which is a pinch-based shortcut method that was initially introduced by Bausa et al. [60,61] for

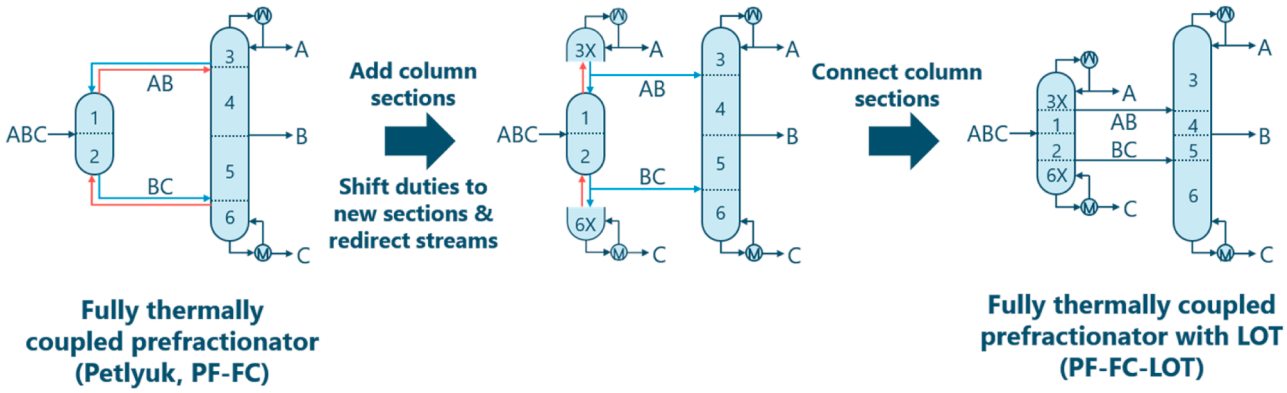

Fig. 5. Development from a Petlyuk configuration to a fully thermally coupled prefractionator with LOT via two side streams.

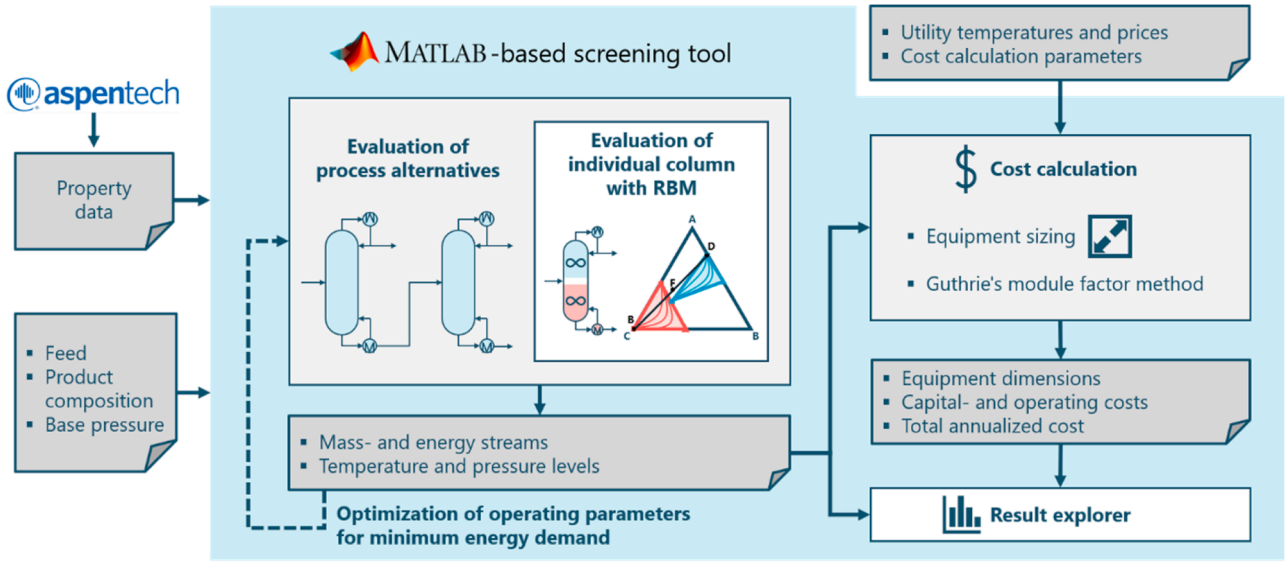

Fig. 6. Schematic of algorithmic framework for shortcut evaluation of energy-integrated distillation processes, after Adami et al. [58].

simple columns and further extended to complex columns with side streams in the rectifying section and/or the stripping section by [62]. The Rectification Body Method only assumes isobaric operation and an infinite number of equilibrium stages and thus can be applied for non-ideal separations without relying on the common assumptions of constant relative volatility or constant molar overflow. It is integrated within the process synthesis software collection of AVT.SVT at RWTH Aachen University [63], which also provides the thermodynamic engine for property calculations.

The screening further determines all relevant mass and energy streams, temperatures and pressures, which together with the MED are further used to determine approximate equipment sizes as well as cost estimates for the operating-, capital- and total annual costs. The approximate equipment sizing builds on the Winn equation [64] and the empirical correlation by Gilliland to calculate the actual number of required equilibrium stages [65], while the cost estimates use utility prices from Turton et al. [66, p. 231] and equipment costs are estimated by Guthrie's method using the correlations reported in the book of [67]. Further details are provided in the Supporting Information in Section S3. We furthermore refer to the recently published article of Adami et al. [58] for a detailed description of the shortcut screening framework. The following subsections provide an outline on the specific process configurations considered in the current study as well as some information on the necessary optimization for the newly considered LOT configurations.

4.1.1. *Overview of considered process configurations*

In order to evaluate the potential of LOT configurations a range of comparable alternative process configurations for the separation of a mixture into three product fractions is considered in this work, covering simple sequences, thermally coupled configurations, LOT configurations and processes with direct HI. This allows for a focused comparison of the LOT configurations, while the shortcut screening tool also enables the evaluation of some multi-effect configurations and heat pump assisted processes, which are explicitly excluded from the current study.

Besides the three simple sequences (direct sequence, indirect sequence, sloppy split), six thermally coupled configurations (SR, SS and the four prefractionator configurations), are evaluated together with an adapted cost estimate for a middle-DWC, which is considered as equipment integrated implementation of the Petlyuk configuration. For the thermally coupled configurations, each bidirectional transfer of liquid and vapor between the coupled columns is approximated by means of subcooled or superheated net streams, which serves as a proper estimate with negligible errors as shown by Navarro et al. [68]. The coupled columns are operated at the same pressure and the involved heat exchangers are neglected for cost calculation, while the remaining heat exchangers fulfill the energy demand of all coupled sections. No additional heat exchanger costs are considered for thermally coupled streams.

From the thermally coupled configurations five additional LOT configurations are derived as introduced by Agrawal [50] and illustrated in Fig. 7.

Furthermore, direct HI is additionally considered for all configurations, except those with horizontal thermal coupling. To achieve HI, the pressure in one of the columns is adjusted such that the distillate temperature of the heat supplying column is raised sufficiently above the bottom temperature of the heat receiving column, considering a fixed approach temperature of 10 K. While the respective heat integration is indicated by two heat exchangers connected via a dashed red line (cf. e.g. Fig. 8), it is modeled with single heat exchanger. Additional intermediate heat exchangers with external utilities are considered to maintain liquid boiling feed conditions at altered pressures and to account for mismatched duties of the heat integrated columns.

For the considered HI configurations each condenser can act as the heat source, while each reboiler of another column can act as the heat sink, and either the pressure in the heat supplying column can be increased (HP: high pressure) or the pressure in the heat receiving column can be decreased (LP: low pressure), leading to four heat integrated combinations for each sequence with two columns as shown for the PF-FC-LOT in Fig. 8. For the sloppy split configuration with three columns, 12 heat integrated variants with a single HI and 18 variants with two HI are considered. In total, 62 heat integrated variants are covered for a total of 77 considered process configurations.

4.1.2. *Optimization of operating parameters*

Some process variants require the optimization of individual degrees of freedom in order to determine the specific MED. This is mostly the case for some configurations with possible distribution of the intermediate boiling product fraction, as e.g. in the sloppy split and the prefractionator. Additionally, for each thermally coupled connection that is replaced by a side stream in an LOT configuration, the respective distribution of the product, which is produced in two adjacent columns becomes an additional degree of freedom. Thus, LOT configurations with multiple side streams require the optimization of multiple degrees

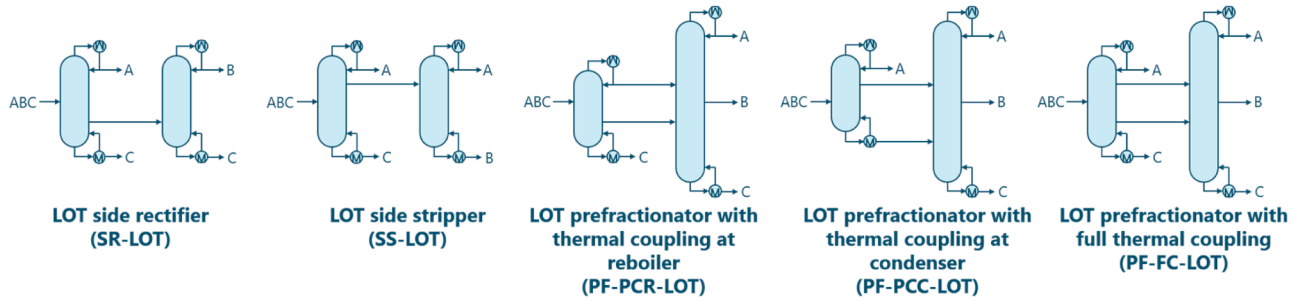

Fig. 7. Flowsheets of five considered LOT process configurations.

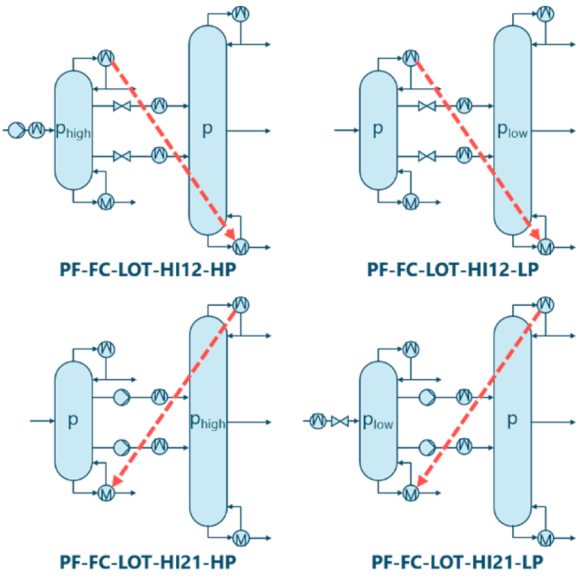

Fig. 8. All four directly heat integrated versions of the PF-FC-LOT. Dashed red arrows indicate the direction of direct heat integration. (HI12: integration from column 1 to column 2; HI21: integration from column 2 to column 1; HP: pressure increase; LP: pressure decrease).

of freedom, making their design more complex. Each of these degrees of freedom can be described by a distribution factor

$$\psi_i = \frac{\dot{n}_{i,\,I}}{\dot{n}_{i,\,I} + \dot{n}_{i,\,II}},\ 0 < \psi_i < 1, \tag{1}$$

defined as the ratio of flowrates for product fraction i distributed in the streams I and II. For the LOT variant of the Petlyuk configuration with two side streams, this results in three independent distribution factors shown in Fig. 9.

The distribution factors are optimized such that the minimum net energy demand of the entire configuration and not just that of the individual columns is obtained. The optimization problem is formulated as

$$\min_{\boldsymbol{\psi}} f(\boldsymbol{\psi}) = \sum_j Q_{B,j},\ \textit{with}\ 0 < \psi_i < 1\ \forall\ i, \tag{2}$$

with $Q_{B,j}$ being the heat duty of all externally heated heat exchangers. It is solved in MATLAB as constrained problem with 'fmincon' using the gradient based interior-point method with a relative abort tolerance of 10^{-3} for the step size with each iteration, starting from an initial value $\psi_i^{(0)} = 0.5$. Preliminary studies have shown that the correct MED is reliably found from this initial value. This is further verified by comparison with the MED of the thermally coupled configurations, as according to Halvorsen and Skogestad [54] the sum of the internal vapor and liquid flows in the sections performing the same separation (so Section 3 and X, as well as 6 and 6X in Fig. 5) are identical to the equivalent thermally coupled configuration. Note that the MED computations indicate that in most cases a range of combinations of distribution factors exists, for which the MED is obtained for the LOT configurations, supporting the expectation that they may provide more operational flexibility than thermally coupled configurations.

4.2. Rigorous superstructure optimization

A rigorous techno-economic optimization is performed with an equilibrium stage superstructure model based on the MESH equations posed in the high-level algebraic modeling language General Algebraic Modeling System (GAMS) in equation-oriented format. The next subsections provide an overview of the individual column models considering side streams and multiple feeds, as well as the connection to column sequences and the required modifications for direct HI or equipment integration for the middle-DWC. Finally, the employed solution procedure for the resulting mixed-integer nonlinear programming (MINLP) problems is described. All models assume isobaric column

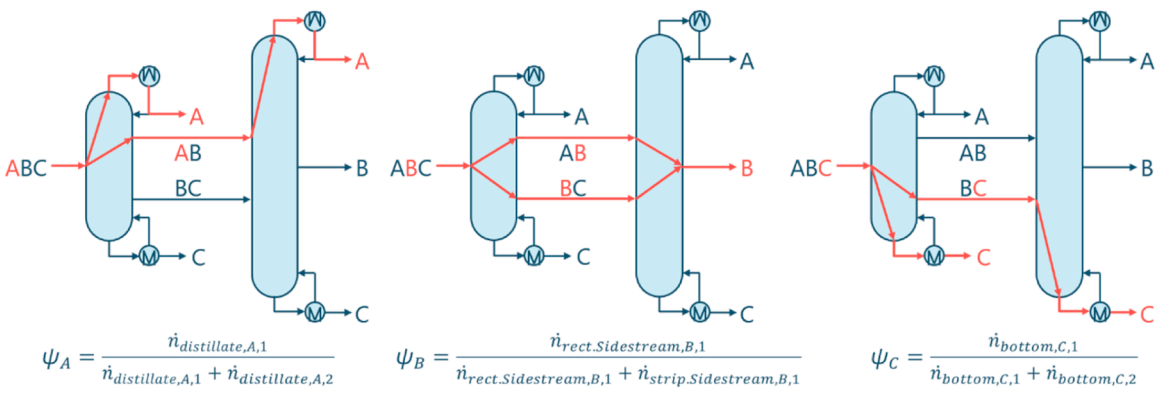

Fig. 9. Degrees of freedom and resulting distribution factors ψ for LOT variant of Petlyuk configuration.

operation and consider inequality constraints for the product purities.

4.2.1. Superstructure model for individual distillation columns

The superstructure model of a simple column with a single feed is described in detail by Skiborowski et al. [59] and Kraemer et al. [31]. Variable sizing of the rectifying and stripping section is enabled by allowing the reflux and boil-up streams to distribute to variable stages in the superstructure, effectively bypassing a series of stages at the top or bottom of the column, which effectively no longer contribute to the separation and are further neglected in the equipment sizing and costing. Additionally, the feed stream may be distributed along the height of the column, adding excess flexibility to the superstructure. The major equations are outlined in this section with modifications to account for the possibility of side streams and multiple feeds, as seen for LOT processes.

The equilibrium stages in the superstructure model for a single column are labeled from 1 to n_{max}, with the first stage representing the condenser and the last representing the reboiler, such that the actual column has a maximum number of $n_{max}-2$ equilibrium stages, depending on the result of the optimization. Each equilibrium stage is described by the MESH equations (mass balances, equilibrium conditions, summation constraints, enthalpy balances), considering all possible entering and leaving streams. The mass balance of a general stage n is stated as

$$\dot{L}_{n-1}\cdot x_{n-1,i} + \dot{V}_{n+1}\cdot y_{n+1,i} + \sum_f \left(\dot{F}_f \cdot z_{F_f,i}\cdot b_{F_f,n}\right) + \dot{R}_n \cdot x_{1,i}\cdot b_{R,n} + \dot{K}_n \cdot y_{n_{\max},i}\cdot b_{K,n} = \dot{L}_n \cdot x_{n,i} + \dot{V}_n \cdot y_{n,i} + \sum_s \left(\dot{S}_s \cdot x_{n,i}\cdot b_{S_s,n}\right), \quad n \in [2, n_{\max}-1], \tag{3}$$

with $\dot{L}_n$ and $\dot{V}_n$ as the molar flow rates and $x_{n,i}$, $y_{n,i}$ the composition of component i for the liquid and vapor phases leaving stage n. $\dot{R}_n$, $\dot{K}_n$, $x_{1,i}$, $y_{n_{max},i}$ are the flow rate and the composition of the reflux and boil-up streams. Extending the established model by Skiborowski et al. [59], $\dot{F}_f$ and $z_{F_f,i}$ are the flowrate and composition of feed f, while $\dot{S}_s$ is the flow rate of side stream s. Thus, the sums over all f and s consider any number of feeds and side streams on a given stage. The superstructure allows variable locations for all feeds, side streams, reflux and boil-up locations to define the effective number of stages of each column section. This is reflected by binary decision variables $b_{F_f,n}$, $b_{S_s,n}$, $b_{R,n}$ and $b_{K,n}$, which determine if the feeds, side streams, reflux or boil-up are entering or leaving stage n. The sum of each decision variable across all stages is set to 1 to fulfill the mass balance:

$$\sum_n b_{F_f,n} = 1 \;\forall f, \quad \sum_n b_{S_s,n} = 1 \;\forall s, \quad \sum_n b_{R,n} = 1, \quad \sum_n b_{K,n} = 1. \tag{4}$$

The enthalpy balance of a general stage is

$$\dot{L}_{n-1}\cdot h^L_{n-1} + \dot{V}_{n+1}\cdot h^V_{n+1} + \sum_f \left(\dot{F}_f \cdot h_{F_f}\cdot b_{F_f,n}\right) + \dot{R}_n \cdot h^L_1 \cdot b_{R,n} + \dot{K}_n \cdot h^V_{n_{\max}}\cdot b_{K,n} = \dot{L}_n \cdot h^L_n + V_n \cdot h^V_n + \sum_s \left(\dot{S}_s \cdot h^L_n \cdot b_{S_s,n}\right), \quad n \in [2, n_{\max}-1], \tag{5}$$

considering specific liquid h^L_n and vapor enthalpies h^V_n, as well as the enthalpies of the feeds h_{F_f}, reflux h^L_1 and boil-up $h^V_{n_{max}}$. The mass and enthalpy balances of the total condenser

$$\dot{V}_2 \cdot y_{2,i} = \dot{D}\cdot x_{1,i} + \dot{R}\cdot x_{1,i}, \tag{6}$$

$$\dot{V}_2 \cdot h^V_2 = \dot{D}\cdot h^L_1 + \dot{R}\cdot h^L_1 - \dot{Q}_{Condenser}, \tag{7}$$

with duty $\dot{Q}_{Condenser}$ and the mass and enthalpy balances of the partial reboiler

$$\dot{L}_{n_{max}-1}\cdot x_{n_{max}-1,i} = \dot{B}\cdot x_{n_{max},i} + \dot{K}\cdot y_{n_{max},i}, \tag{8}$$

$$\dot{L}_{n_{max}-1}\cdot h^L_{n_{max}-1} + \dot{Q}_{Reboiler} = \dot{B}\cdot h^L_{n_{max}} + \dot{K}\cdot h^V_{n_{max}}, \tag{9}$$

with duty $\dot{Q}_{Reboiler}$ are defined similarly. The model furthermore considers the column mass balance

$$\sum_f \dot{F}_f = \dot{D} + \dot{B} + \sum_s \dot{S}_s, \tag{10}$$

with $\dot{D}$ and $\dot{B}$ as distillate and bottom flow rate and the column enthalpy balance

$$\sum_f \left(\dot{F}_f \cdot h_{F_f}\right) + \dot{Q}_{Reboiler} = \dot{D}\cdot h^L_1 + \dot{B}\cdot h^L_{n_{max}} + \sum_s \sum_n \left(\dot{S}_{s,n}\cdot h^L_n \cdot b_{S_s,n}\right) - \dot{Q}_{Condenser}. \tag{11}$$

Summation equations are considered for all liquid and vapor mole fractions:

$$\sum_i x_{n,i} = 1 \;\forall\, n, \quad \sum_i y_{n,i} = 1 \;\forall\, n. \tag{12}$$

As indicated in Fig. 10, the enthalpies as well as the vapor-liquid equilibrium computations are performed by means of external equations, considering rigorous thermodynamic models. The external equations are introduced in the form of a dynamic link library (DLL) whereas in each iteration of the optimization, a set of variables z is transferred from GAMS to the external function which returns the results of the evaluation of the external equations $e(z)$ and the gradients of the external equations $\frac{\partial e(z)}{\partial z}$. This can be considered as a reduced space formulation of the optimization problem, limiting the number of variables and equations handled by GAMS [59]. The specific models used in the current study are further described in Section 5, while the respective equations and property parameters are summarized in the Supporting Information in Section S1 and S2.

4.2.2. Connection of individual columns to configurations

For all configurations individual columns need to be connected as further described for the case of two individual distillation columns ($c = 1, 2$), that are connected via their material and energy streams. Selected product streams from column 1 may either exit the two-column sequence as final products or serve as feed streams to the second column. In the latter case, the mass flow rate, component mole fractions and specific enthalpy of the product stream of column 1 are set to the corresponding feed stream of column 2, thus enforcing full material- and energy-consistency across the intercolumn connection. If the distillate D of column 1 is the feed stream F of column 2, then

$$\dot{D}_1 = \dot{F}_2, \quad x_{D,1,i} = x_{F,2,i}, \quad y_{D,1,i} = y_{F,2,i}, \quad h^L_{D,1} = h^L_{F,2}, \quad h^V_{D,1} = h^V_{F,2} \tag{13}$$

It therefore depends on the modeled configuration which streams are routed internally versus externally. Although each individual-column model is capable of accommodating multiple feeds and side draws, in certain configurations the column models reduce to simpler cases with a single feed and no side draws.

Overall mass and energy balances for the entire configuration are not explicitly required, they exist implicitly via the specifications of the connected columns. The total external heating duty

$$\dot{Q}_{Heating,ext} = \sum_c \dot{Q}_{Reboiler,c} \tag{14}$$

and total external cooling duty

$$\dot{Q}_{Cooling,ext} = \sum_c \dot{Q}_{Condenser,c} \tag{15}$$

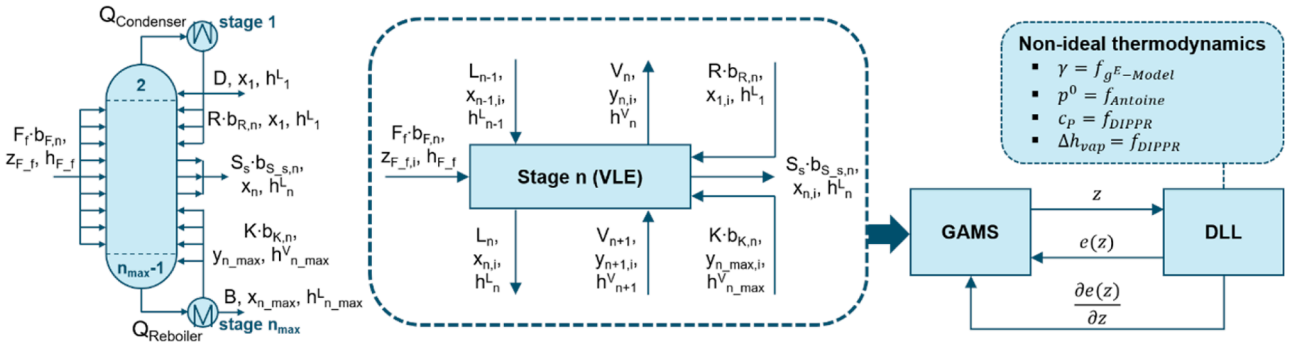

Fig. 10. Superstructure of individual distillation column and conjunction of GAMS with external function - after Waltermann and Skiborowski [69] - modified for multiple feeds and side draws.

are further determined.

4.2.3. Modifications for direct heat integration

While Waltermann and Skiborowski [69] already introduced models for thermally coupled configurations and sequences with direct HI, the respective modifications are employed and extened in this work to enable HI by pressure increase or decrease in one of the columns and consideration of heat exchangers for preconditioning of the feed into every column, such that liquid boiling feed conditions are always possible when the pressure of streams is altered, including the LOT configurations.

As for the shortcut screening, the pressure of one column is adjusted in order to ensure a sufficient temperature difference for heat transfer, while the pressure of the other column remains constant. Since the necessary setpoint pressures to enable heat integration with a sufficient approach temperature were already determined in the shortcut screening, these are specified for the rigorous optimization, instead of determining the adjusted pressure level based on a variable operating pressure in one column and an additional constraint for the minimum approach temperature. This improved numerical robustness of the optimization, as each vapor liquid equilibrium is affected by the modification of the operating pressure. Pumps and throttle valves are further assumed as isenthalpic, only modifying the pressure of affected streams, considering that they do not significantly affect the MED.

The energy balances for the condenser of the heat rejecting column

$$\dot{V}_2 \cdot h_2^V = \dot{D} \cdot h_1^L + \dot{R} \cdot h_1^L - \dot{Q}_{Condenser} + \dot{Q}_{HI}, \tag{16}$$

and the energy balance of the reboiler of the heat receiving column

$$\dot{L}_{n_{max}-1} \cdot h_{n_{max}-1}^L + \dot{Q}_{Reboiler} + \dot{Q}_{HI} = \dot{B} \cdot h_{n_{max}}^L + \dot{K} \cdot h_{n_{max}}^V, \tag{17}$$

are modified to account for the integrated duty $\dot{Q}_{HI}$ exchanged in a single heat exchanger for HI. A remaining condenser and reboiler are considered to compensate for potential differences in the respective duties of the integrated columns.

To avoid subcooled or superheated feeds entering columns at altered pressure levels leading to subpar thermodynamic performance, each feed stream entering a column is potentially passing an intermediate heat exchanger for preconditioning. This feed preconditioner allows adjustment of the thermal state of the feed such that saturated liquid conditions can be achieved at the column operating pressure, regardless of the pressure at the feed origin.

Depending on the enthalpy difference at liquid boiling conditions caused by the pressure mismatch, each preconditioner can either add or remove heat $\dot{Q}_{Preconditioner,f}$ via external utilities, described by an enthalpy balance

$$\dot{Q}_{Preconditioner,f} = \dot{F}_f \cdot \left(h_{F_f,destination} - h_{F_f,origin} \right) \tag{18}$$

with $h_{F_f,origin}$ as the specific enthalpy of feed stream f at its original conditions and $h_{F_f,destination}$ as the specific enthalpy when entering the respective column. While this formulation enables feed preconditioning as far as beneficial, it does not enforce liquid boiling feed conditions.

The stage-wise and overall column energy balance are modified such that the preconditioned feed enthalpy $h_{F_f,destination}$ is used to ensure thermodynamic consistency when using preconditioned feed streams. In addition, preconditioners providing heat ($\dot{Q}_{Preconditioner,f} > 0$) are considered for the overall external heating

$$\dot{Q}_{Heating,ext} = \sum_c \dot{Q}_{Reboiler,c} + \sum_c \sum_f \dot{Q}_{Preconditioner,c,f} \tag{19}$$

and preconditioners removing heat ($\dot{Q}_{Preconditioner,f} < 0$) for the external cooling duty

$$\dot{Q}_{Cooling,ext} = \sum_c \dot{Q}_{Condenser,c} + \sum_c \sum_f \dot{Q}_{Preconditioner,c,f} \tag{20}$$

4.2.4. Modifications for middle dividing wall column

The middle-DWC model builds on the representation of the Petlyuk configuration, while adapting the sizing and cost calculations to account for the single-shell implementation. Unlike our previously presented optimization strategies for DWC [43,69], which pursue a sequence of model reformulations for the initialization of the DWC model, starting from a sequence of simple columns, such as the sloppy split sequence for the middle-DWC, the current work performs a reformulation builds on the previously introduced model for multiple feed streams and side streams. Thus, the middle-DWC model is initialized on the basis of a sequence of a simple column and a subsequent column that receives both products of the first column as feed streams, while returning a reflux and boil-up stream to the first column and producing three product streams, skipping some steps in the initialization sequence.

Thus, the top vapor stream of the first column and the bottom stream serve as feed streams to the second column, while the liquid side stream leaving the upper feed stage of the second column acts as reflux to the first column. Similarly, the vapor side stream leaving the lower feed stage of the second column acts as the boil-up stream for the first column. This connection is established by modifying the balance equations of the condenser and reboiler stages of column $c = 1$ are modified to account for the mass and enthalpy flows that arrive from column $c = 2$. The modified balances for the first stage of the first column, receiving the liquid side stream from the second column, are

$$\dot{V}_{2,c=1} \cdot y_{2,c=1,i} + \sum_{n_{c=2}} \left(\dot{S}_{s=1,n,c=2} \cdot x_{n,c=2,i} \cdot b_{S_1,c=2,n} \right) = \dot{D}_{c=1} \cdot y_{1,c=1,i}, \tag{21}$$

$$\dot{V}_{2,c=1} \cdot h_{2,c=1}^V + \sum_{n_{c=2}} \left(\dot{S}_{s=1,n,c=2} \cdot h_{n,c=2}^L \cdot b_{S_1,c=2,n} \right) = \dot{D}_{c=1} \cdot h_{1,c=1}^V, \tag{22}$$

and the balances of the last stage of the first column, receiving the vapor side stream from the second column, are

$$\dot{L}_{n_{max}-1,c=1}\cdot x_{n_{max}-1,c=1,i}+\sum_{n_{c=2}}\left(\dot{S}_{s=2,n,c=2}\cdot y_{n,c=2,i}\cdot b_{S_2,c=2,n}\right)=\dot{B}_{c=1}\cdot x_{n_{max},c=1,i}, \tag{23}$$

$$\dot{L}_{n_{max}-1,c=1}\cdot h^{L}_{n_{max}-1,c=1}+\sum_{n_{c=2}}\left(\dot{S}_{s=2,n,c=2}\cdot h^{V}_{n,c=2}\cdot b_{S_2,c=2,n}\right)=\dot{B}_{c=1}\cdot h^{L}_{n_{max},c=1}. \tag{24}$$

The decision variables of the first column for reflux (boilup) now determine where the transferred liquid (vapor) enters the column. To ensure that each pair of counter-directed streams interacts with the same equilibrium stage of column 2, a single set of binary decision variables is used for both members of the pair:

$$b_{S_1,c=2,n}=b_{F_1,c=2,n} \tag{25}$$

$$b_{S_2,c=2,n}=b_{F_2,c=2,n} \tag{26}$$

The energy and mass balances for general stages are modified accordingly. The final model similarly represents a set of horizontally coupled columns where the number of equilibrium stages in all sections of both columns are variable by adapting the location of the reflux and the boil-up stream and all feed and side draw locations, while the intermediate boiling product is drawn as liquid side stream from the second column.

4.2.5. Sizing and cost estimation

The techno-economic optimization pursues a minimization of the total annualized costs TAC, which are basically calculated identical to the shortcut screening (cf. Supporting Information Section S3), but considering the specific sizing that is determined from the superstructure optimization, for which the actual number of equilibrium stages in each column is determined. The specific stage number

$$n_{actual}=n_{max}-\sum_{n}b_{R_{Sumn}}-\sum_{n}b_{K_{Sumn}}+2, \tag{27}$$

is calculated by subtracting all stages above the reflux tray and all stages below the boil-up tray from the maximum number of stages n_{max} [31]. The variable

$$b_{R_{Sumn}}=\sum_{j\geq n}^{n_{max}}b_{R,j} \tag{28}$$

is equal to 1 for all stages from the boil-up tray to the reboiler and the variable

$$b_{K_{Sumn}}=\sum_{j=1}^{j\leq n}b_{K,j} \tag{29}$$

for all stages from the condenser to the reflux tray. Therefore n_{actual} is corrected by (+2) to make-up for the boil-up and reflux tray.

The diameter that results for a specified F-Factor F

$$D_{Col,n}=\sqrt{\frac{4\cdot V_n}{\pi\cdot F}\sqrt{\frac{R\cdot T_n\cdot\sum_i y_{n,i}\cdot M_i}{p}}}. \tag{30}$$

for a specific stage n is calculated according to Douglas [65] from the gas load on each stage . The final diameter of the column shell is further determined as $max_n D_{Col,n}$, for all equilibrium stages aside from condenser and reboiler stages to provide a consistent column diameter that assures that the specified F-Factor is not exceeded.

For the sizing of the middle-DWC is more complex, as the height of the middle part of the DWC separated by the dividing wall needs to be determined consistently for both sides, and the diameter for the column shell needs to account for the parallel sections. Therefore, the individual diameters $D_{middle-DWC,r}$ and $D_{middle-DWC,l}$ for the right- and left side of the divided section are calculated by Eq. (30) and the diameter of the combined shell $D_{middle-DWC}$ is determined by a lower bound on the basis of the cross-sectional equivalent diameter

$$D_{middle-DWC}\geq\sqrt{D^2_{middle-DWC,r}+D^2_{middle-DWC,l}} \tag{31}$$

of the parallel sections calculated similarly to Dejanović et al. [41], as well as a lower bound for the minimum diameters for the non-divided sections m

$$D_{middle-DWC}\geq D_{middle-DWC,m}. \tag{32}$$

The number of stages of the middle-DWC n_{mDWC} is the larger number of stages from the left or right section in addition to the number of stages of the non-divided sections:

$$n_{mDWC}\geq\sum_{m}n_{actual,m}+n_{actual,l}, \tag{33}$$

$$n_{mDWC}\geq\sum_{m}n_{actual,m}+n_{actual,r}. \tag{34}$$

Considering the additional costs for the dividing wall and the more complicated construction compared to a conventional column, a surcharge factor of 20 % [41] is added to the investment costs for the column shell. While this approach does not impede unequal stage numbers on both sides of the dividing wall, there is also no economic incentive to eliminate stages on a single side of the DWC, given that this would reduce separation efficiency without reducing the associated investment costs.

4.2.6. Solution strategy

Since all process variants possess many discrete as well as continuous variables and nonlinear expressions, the resulting MINLP problems are challenging to solve. Based on existing experience with the optimization of distillation processes [24,31,59,70] a polylithic solution approach [24,31,59,70] is pursued for the model initialization and reformulation, solving the resulting MINLP problem by means of a successively relaxed continuous reformulation as a series of constrained/penalized NLP problems, as introduced by Kraemer et al. [31]. In order to improve the computational robustness, an automated stepwise initialization procedure is employed, with each subsequent step increasing the complexity of the problem while providing good initial values for the next step. The initialization and solution strategy presented in Fig. 11 is based on the approach by Waltermann and Skiborowski [69].

The required input includes feed and product specifications, the thermodynamic model and parameters for cost calculation. In addition, the maximum number of equilibrium stages of the individual columns, as well as initial values for the feed and side stream stages must be specified, defining the initial superstructure. In order to provide reasonable values for the definition of the superstructure, the estimated number of equilibrium stages, side stream compositions and flow rates obtained via the shortcut screening are utilized to serve as initial estimates to aid convergence.

At first each individual column model is initialized in a series of steps, keeping all binary decisions fixed. The first step of the initialization performs a flash calculation of the feed, to provide initial compositions and temperatures for each stage. Next, the full column model is solved for material-, equilibrium and summation (MES) equations before the enthalpy balances (MESH) are included, without considering a specific objective function, while satisfying purity constraints obtained via the shortcut calculations for the products. Finally, the whole column model is optimized for determining the minimum reboiler duty.

After the first column has converged, the same procedure is applied to the second column, using the products of the first column as its feed. The individual stand-alone column models are subsequently connected

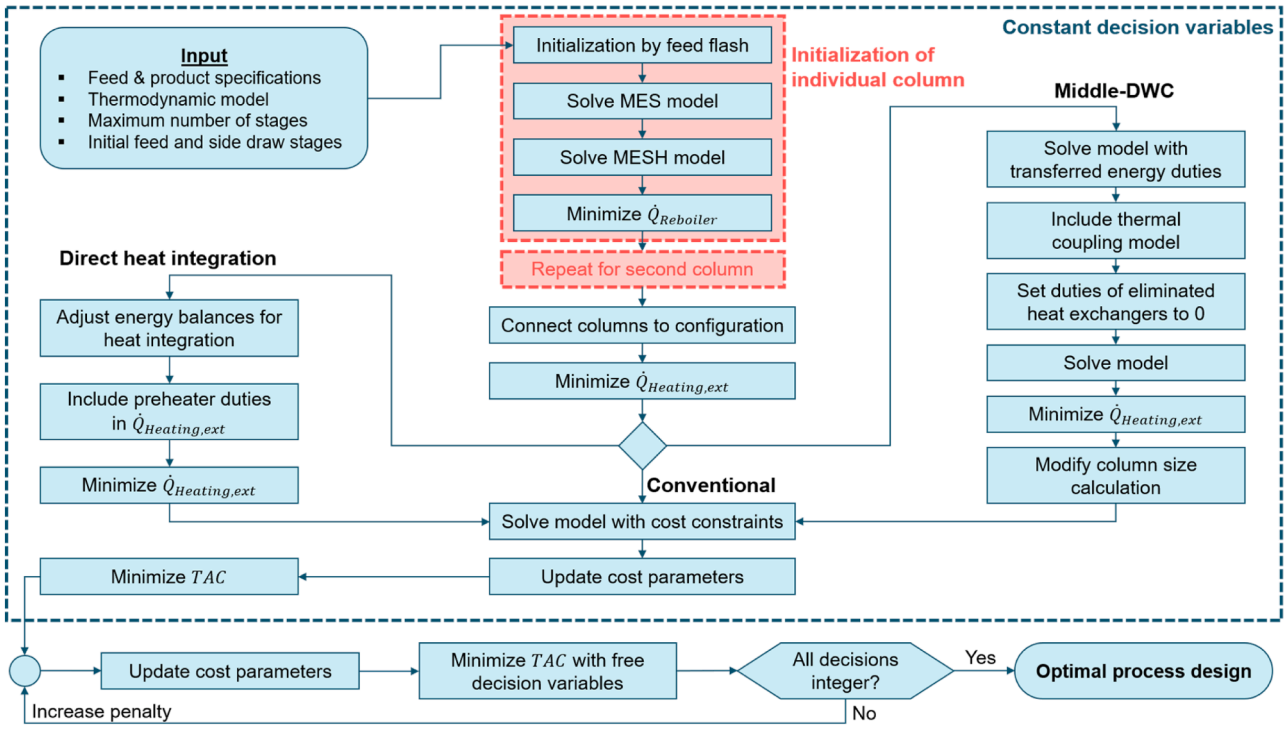

Fig. 11. Initialization and solution procedure for conventional sequences, sequences with heat integration and the middle-DWC.

to generate a joint model of the specific configuration without energy-integration, which is first optimized for minimum external heating duty, with purity and recovery constraints enforced only on the final product streams. Depending on the configuration under consideration, the model equations are furthermore automatically adapted to incorporate direct HI according to the description in Section 4.2.3, or to impose thermal coupling according to the description in Section 4.2.4. The derived model is further re-optimized for minimum external heat duty, prior to adding the cost correlations and solving the model for minimum TAC.

Finally, the binary decision variables are relaxed to continuous variables between 0 and 1, while additional Fischer–Burmeister functions are introduced as penalty terms to the objective. Deviations from binary values are initially tolerated and subsequently penalized with increasing penalty weights, such that a MINLP solution is obtained after several consecutive solutions of the NLP while iteratively increasing the weights by a factor of ten. The iterations terminate once all decision variables have converged to binary values for each stage of the column.

Since module- and correction-factors for the cost estimation are also size-dependent, the specific cost parameters are updated iteratively after each successful solution during the sequence of optimization steps, in order to avoid a smoothing of the discrete step changes in the cost parameters. Utility choice with corresponding temperatures and costs are likewise updated according to the prevailing temperature levels.

5. Case study

In order to evaluate the potential of the LOT configurations, a well-known case study for the separation of a liquid feed into three products is considered as case study. The specific separation problem is the well-studied separation of a benzene, toluene, and p-xylene mixture [40, 71–74], for which a saturated liquid feed at a flow rate of 10 mol/s (=0.92 kg/s) at a reference pressure of 1 atm is considered. The nonideal behavior of the liquid phase is captured using the NRTL activity coefficient model, while the Redlich-Kwong equation of state accounts for vapor-phase nonidealities at elevated pressures resulting from direct HI. Additionally, the extended Antoine equation and DIPPR correlations provide the necessary data for specific heat capacities and heats of vaporization. The utilized thermodynamic property models and respective property parameters are presented in Section S1 and S2 of the Supplementary Material.

First, the shortcut screening is employed to evaluate the performance of LOT processes without and with HI against competing alternatives, particularly the middle-DWC for an equimolar feed composition, as has been studied in several publications that particularly focused on the design of DWC. Subsequently, a systematic analysis is conducted across a range of feed compositions to determine both the net MED and the TAC for each configuration, in order to screen for the maximum benefits enabled by LOT configurations. Having identified the most promising application cases and the best performing process configurations in the screening phase, finally, a rigorous techno-economic optimization is performed for these process configurations to validate the expectations from the shortcut screening and to enable a more detailed analysis of these key configurations. This comparison particularly includes the optimal design and operating parameters for the middle-DWC and heat integrated LOT processes, confirming their excellent saving potential.

5.1. Shortcut screening for an equimolar feed

Starting with the separation of an equimolar saturated liquid feed, the shortcut screening evaluates the net MED for the considered 77 process configurations with a wall-clock time of under three minutes, when executed on a PC with an Intel i7–8700 CPU using MATLAB R2024b through computation on 6 parallel workers making use of the Parallel Computing Toolbox. The resulting net MED of 73 of these configurations are summarized in the bar diagram in Fig. 12, which excludes four of the heat-integrated sloppy split variants with larger pressure variations, since the temperature levels of the heat exchangers are not compatible with the selected external utilities or the lower threshold for the column pressures at 50 mbar to avoid deep vacuum operation was violated.

While each bar in Fig. 12 represents the net energy demand of one of the remaining 73 configurations, the thermally coupled configurations (dark blue), LOT configurations (light blue) and LOT + HI (red)

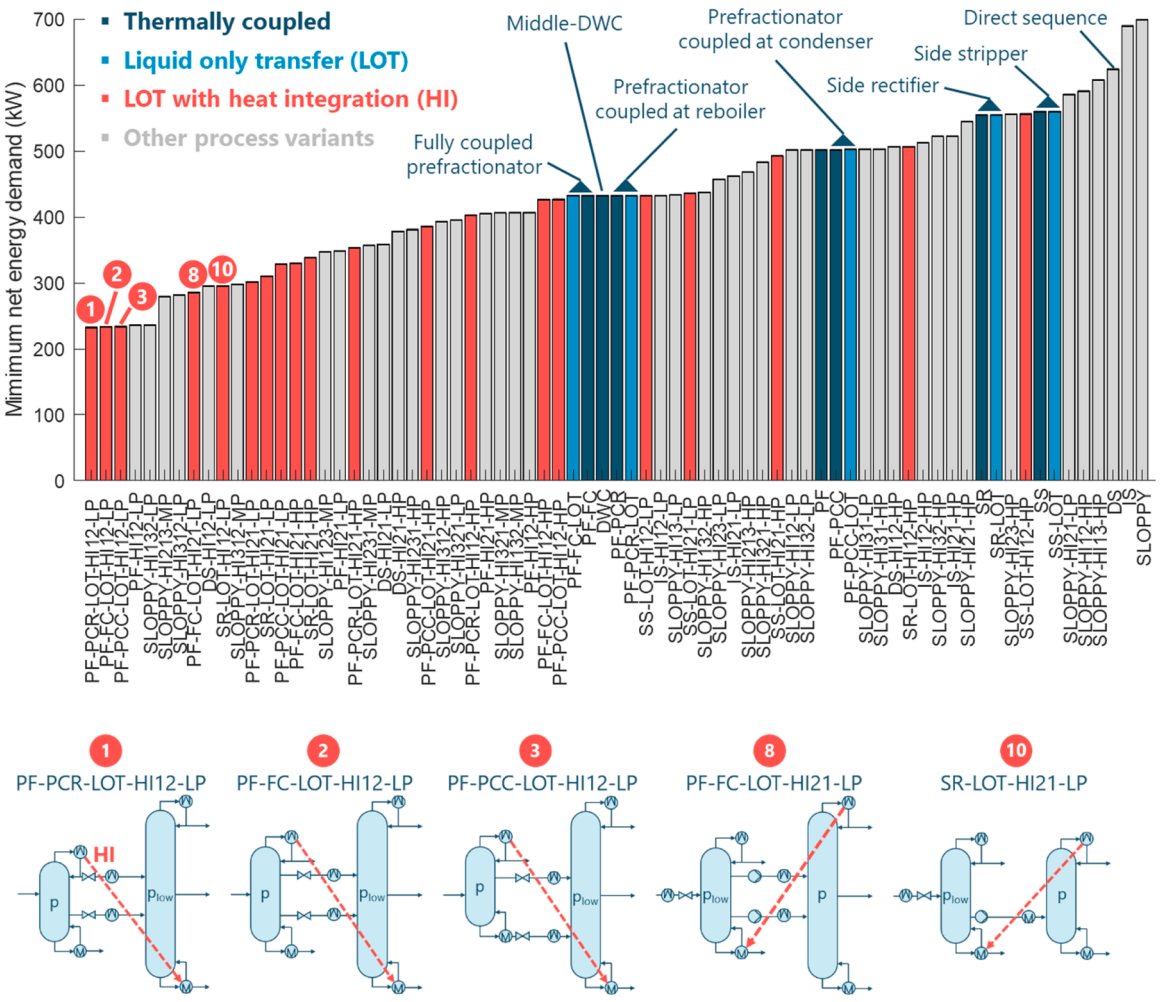

Fig. 12. Net MED of feasible sequences with highlighted sequences and flowsheets of interest. Each bar represents a unique configuration. We refer to the nomenclature at the beginning of this work for interpretation of the configuration identifiers.

configurations are highlighted in specific color code. Notably, the net MED of thermally coupled sequences and their corresponding LOT configurations is basically identical, with numerical differences below 1 %, which is in the range of abort tolerance of the optimization. This indicates the effectiveness of the local optimization to successfully identify the ideal distribution factors for thermodynamically equivalent operation. This consistency was is also observed for other feed compositions, as investigated in Section 5.2.

The best simple sequence is the direct sequence, which has the third highest energy demand of 625 kW, while the middle-DWC and equivalent fully coupled prefractionator configurations achieve energy savings of 30 % with a net MED of 433 kW, which is the expected saving potential that was reported in various publications [23,24]. However, with these savings the middle-DWC ranks only at position #36 with several heat integrated simple configurations, but especially the heat integrated LOT configurations providing significantly lower net MED.

The top three variants with the lowest net MED, as highlighted in Fig. 12, all make use of LOT with HI based on the prefractionator with thermal coupling at the reboiler, the condenser, and full thermal coupling. These three configurations all require a net MED of around 234 kW with energy savings of 63 % over the direct sequence. Interestingly, the largest energy savings for this feed composition are obtained with only one and not two side-streams. The configurations with the 4th and 5th lowest net MED are a PF-HI configuration and a sloppy split for which all three columns are heat integrated. While these configurations only require a slightly increased MED, they all save about 40 % of the net MED of the middle-DWC. The best LOT-HI configuration with a single side stream, which is not based on the prefractionator, is the SR-LOT-HI21-LP (ranking at position #10). It still achieves 53 % energy savings over the direct sequence, which is still more than 30 % less than the middle-DWC. The best HI variant using pressure increase (PF-FC-LOT-HI21-HP) ranks at position #15 with 47 % savings over the direct sequence.

While most LOT-HI configurations in this comparison, whether employing a single or two side-streams and utilizing either pressure reduction or pressure increase, have lower net MED requirements compared to the middle-DWC, it should be noted that this is not generally the case for every LOT-HI variant. Duanmu and Sorensen [75] did e.g. consider only the PF-FC-LOT-HI12-HP configuration with two side streams as in an optimization-based design study that investigates several other configurations, including the middle-DWC and modifications with heat pumps. The LOT configuration with direct HI does neither provide energy nor cost savings compared to the middle-DWC when studying the separation of an almost equimolar mixture of benzene, toluene and o-xylene, instead of p-xylene. To elucidate this limitation, we have applied the shortcut screening for the respective system and compiled the results similar to Fig. 12 in Figure S1 in Section S4 of the Supplementary Material. The shortcut screening confirms that the LOT-HI sequence selected by Duanmu and Sorensen [75] has a 10.5 % higher net MED than the middle-DWC for this separation. However, several other LOT-HI configurations provide a significantly lower net MED, with the PF-PCC-LOT-HI12-LP yielding net savings of 42.9 %

compared to the middle-DWCand ranks within less than 1 % of the best performing configuration. These observations highlight the value of a fast and comprehensive screening of many process variants on a case-specific basis, to avoid missing out on promising variants in a time-intensive optimization with rigorous models.

5.2. Extended shortcut screening for varying feed compositions

For a broader assessment of the potential energy and cost savings of LOT configurations a systematic analysis of all 77 sequences is conducted for 171 equally distributed feed compositions, providing a sensitivity assessment regarding the effect of the distribution of low, intermediate and heavy boiler in the feed. The resulting evaluation of 13,167 feed and process combinations is performed in less than 6 h of wall-clock time.

The configurations with the lowest net MED are shown in Fig. 13 (left) for the range of individual feed compositions illustrated by individual symbols in the Gibbs diagram. For most considered feed compositions, LOT-HI configurations require the least net energy. Only for 11 % of feed compositions the PF-HI12-LP or a sloppy split with two HI links provide lower net MED, however only with a negligible difference of ~1 % difference to one of the LOT-HI configurations. For a about half the feed compositions, partially coupled LOT-HI variants of the prefractionator with only a single side stream outperform fully coupled LOT-HI processes, supporting the previous observation that two side streams are not required for the largest savings. These configurations exploit a lower temperature lift for heat integration as they do not require an integration between the condensation of the low boiler and the evaporation of the heavy boiler. The net MED of the first and second best configurations lie within 2 % for about 85 % of the considered feed composition, indicating there are several similarly viable process options in most situations.

A direct comparison of the best performing configuration for a given feed with the middle-DWC in Fig. 13 (right) confirms that heat integrated LOT processes significantly outperform the middle-DWC across the board by at least 15 %, but up to over 55 % lower net MED, with the largest savings towards higher feed concentrations of medium and high boiler.

The substantial energy savings exceeding 50 % warrant a closer look as they extend beyond the typical savings of simple heat integration. While perfectly matching the reboiler duty of one column with the condenser duty of another can, at best, reduce the configuration's energy demand by 50 %, the more extensive savings observed in fully thermally coupled LOT-HI configurations compared to the middle-DWC stem from a combination of effects. One aspect is the beneficial effect of lower operating pressures on the relative volatility, making the separation inherently easier and thus reducing the intrinsic energy demand. To be fair, this benefit could also be exploited to some extend by operating the middle-DWC at a lower operating pressure. Furthermore, the product streams from these lower-pressure columns exit the system at reduced temperatures, transporting less sensible heat, which does not to be supplied to achieve the desired product conditions. Therefore, products from a benchmark configuration like the middle-DWC can exit at higher temperatures with more sensible heat that could be exploited by further heat integration, e.g. for pre-heating the feed from ambient conditions or integration with other process streams. The current evaluation does not cover this, which is considered reasonable given that products streams would otherwise require cooling for storage if heat integration is not further considered. While both of these advantages are not exclusive to LOT or HI configurations but directly result from modifying columns pressures in the screening, they are effectively exploited by them. As additional step, an identical control volume could be considered by accounting not only for identical product compositions but also thermal states of each entering and leaving stream, which is however out of scope for the current study.

To obtain a more in-depth insight into the possible savings of the individual LOT-HI configurations, the net MED of six promising LOT-HI variants are compared to the middle-DWC for each feed composition in Fig. 14. Net energy savings of over 50 % can be obtained with multiple configurations based on the prefractionator with one or two side streams.

The LOT configuration of the side rectifier with HI from the first to the second column also enables savings of over 50 % compared to the middle-DWC for high concentrations of heavy boiler and roughly equal amounts of light and medium boiler in the feed and performs better across the board than the same configuration with HI in the reverse direction studied previously by Skiborowski [29] and Adami et al. [30]. For feed compositions with high fractions of light or medium boiler however, both displayed SR-LOT-HI configurations show little to no advantage over the middle-DWC, opposed to the LOT-HI configurations based on the prefractionator, as their performance saving potential is less dependent on the feed composition. For most feed compositions, several of the shown variants exhibit very similar energy saving potential over the middle-DWC.

To evaluate whether the observed energy savings can translate into cost savings, Fig. 15 presents the best-performing configurations in terms of the TAC estimates from the shortcut results for different feed compositions. 17 distinct configurations achieve the lowest TAC for individual feed compositions, highlighting that no single configuration is superior, even for the separation of the same mixture. This general conclusion is in line with the results of Brüggemann and Marquardt [76], who however only investigated (partially) thermally coupled configurations. Overall, LOT processes emerge as the most cost-effective for 46 % of the feed compositions studied, in most cases in combination with

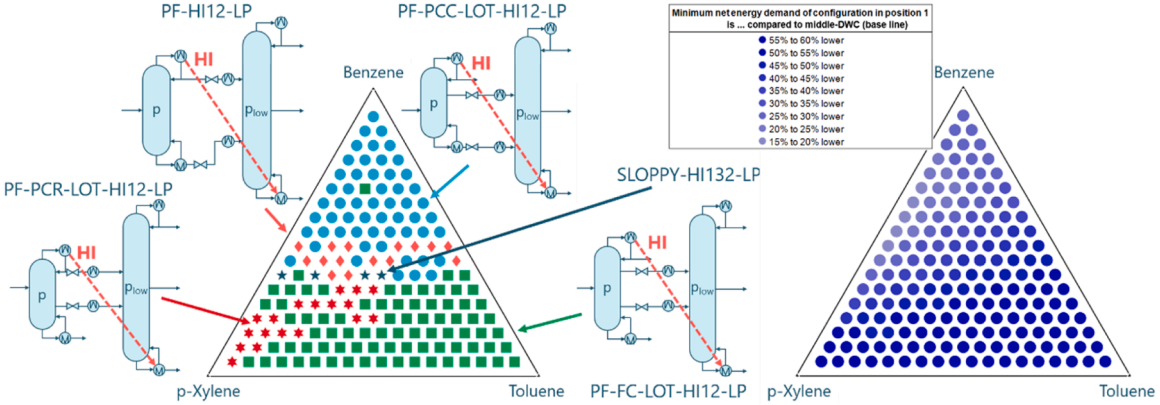

Fig. 13. Best configurations regarding minimum net energy demand (left) and difference compared to middle-DWC (right) for separation of different feed compositions, considering all feasible configurations.

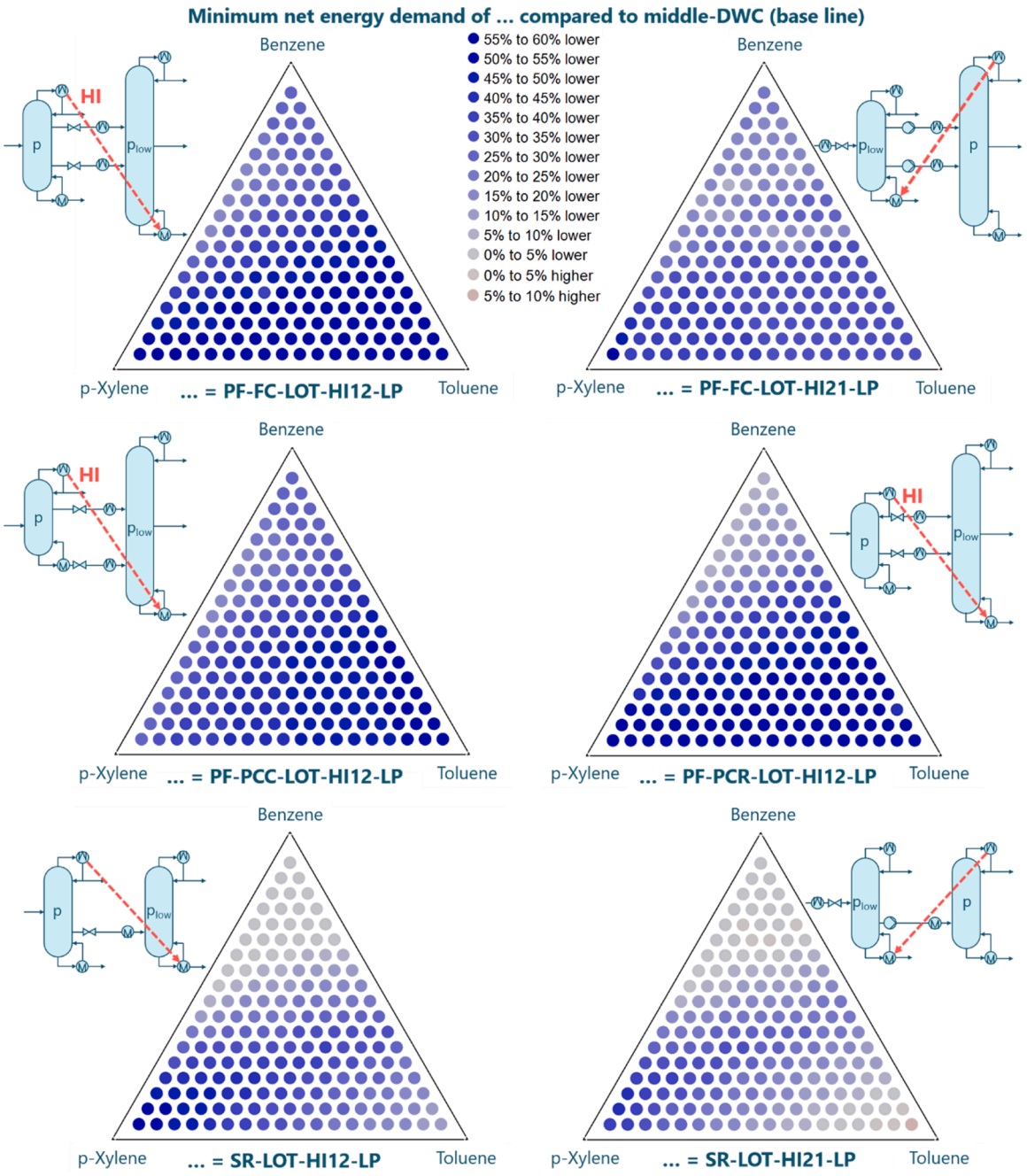

Fig. 14. Difference in minimum net energy demand of selected LOT-HI configurations compared to middle-DWC for separation of different feed compositions.

HI. For feeds with high concentrations of high-boiler, SR-LOT-HI variants exhibit the lowest TAC, while prefractionator-based LOT configurations excel for many other compositions. In contrast, heat-integrated configurations without side streams are generally most economical when the feed is rich in intermediate-boiling components. Notably, a side stripper-based LOT-HI configurations rank first only for a single feed composition, and the middle-DWC only achieves the lowest TAC for 9 feed compositions, with low amounts of medium boiler. Moreover, the degree of cost savings over the middle-DWC increases as the feed composition deviates from these conditions, as illustrated in Fig. 15 (right). Among all configurations, the SR-LOT-HI12-LP achieves the largest TAC savings of over 35 % relative to the middle-DWC for feed compositions with particularly high concentrations of high-boiling components.

In case vacuum operation is to be avoided as it requires an additional vacuum system, which is not reflected in the employed cost calculations, LOT-HI configurations have the lowest net MED for most feed compositions as shown in Fig. 16 (left), except for a heat integrated sloppy split with two direct HI links, which performs best for high concentrations of medium boiler. Energy savings over the middle-DWC are possible for every feed composition, reaching over 40 % for high concentrations of high and medium boiler (see Fig. 16 (right)).

An evaluation of the TAC estimates, excluding configurations with columns operating under vacuum conditions (see Fig. 17), reveals trends similar to those observed when vacuum processes are considered. In this case, 14 different configurations emerge as lowest TAC over the range of feed compositions, with LOT configurations as the most economical again for 46 % of the compositions, in most cases in the form of LOT-HI. In contrast, the middle-DWC has the lowest TAC for 22 % of feed compositions.

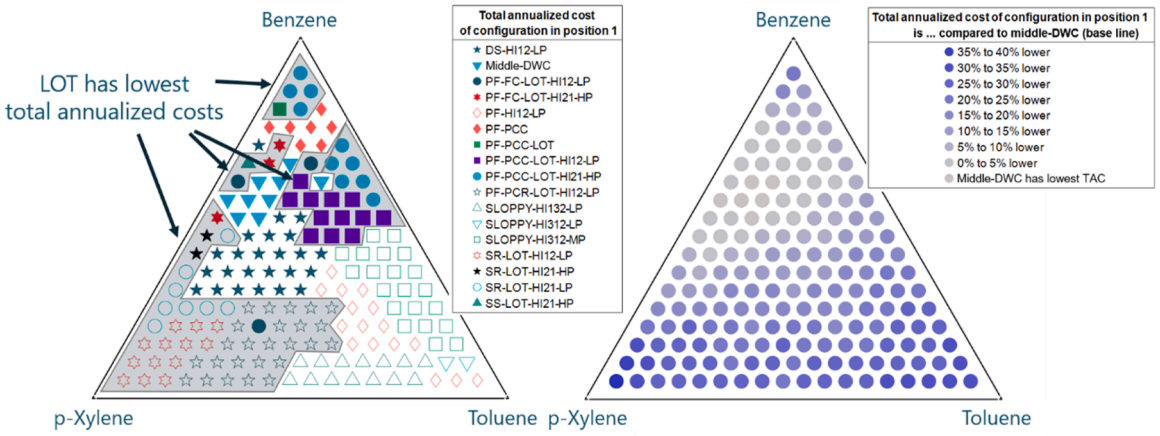

Fig. 15. Best configurations regarding total annualized cost (left) and difference compared to middle-DWC (right) for separation of different feed compositions, considering all feasible configurations. We refer to the nomenclature at the beginning of this work for interpretation of the configuration identifiers.

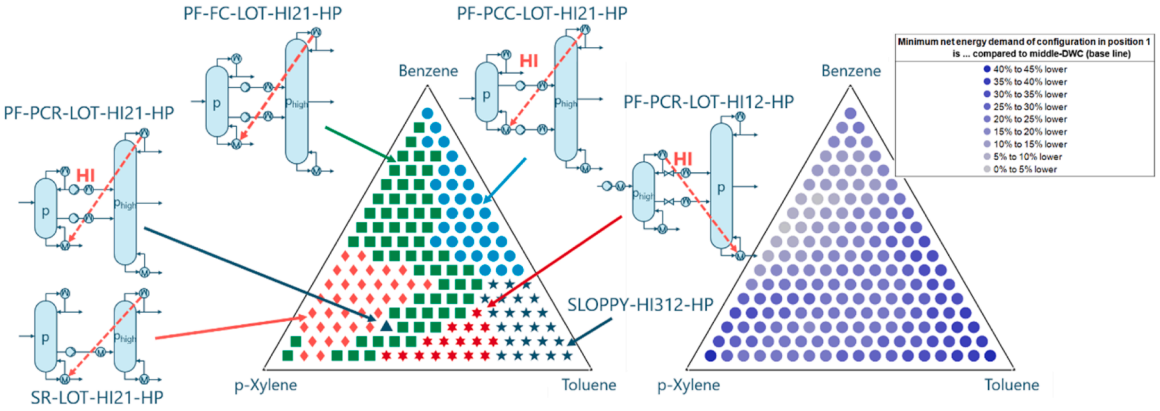

Fig. 16. Best configurations regarding minimum net energy demand (left) and difference compared to middle-DWC (right) for separation of different feed compositions, excluding configurations with vacuum operation.

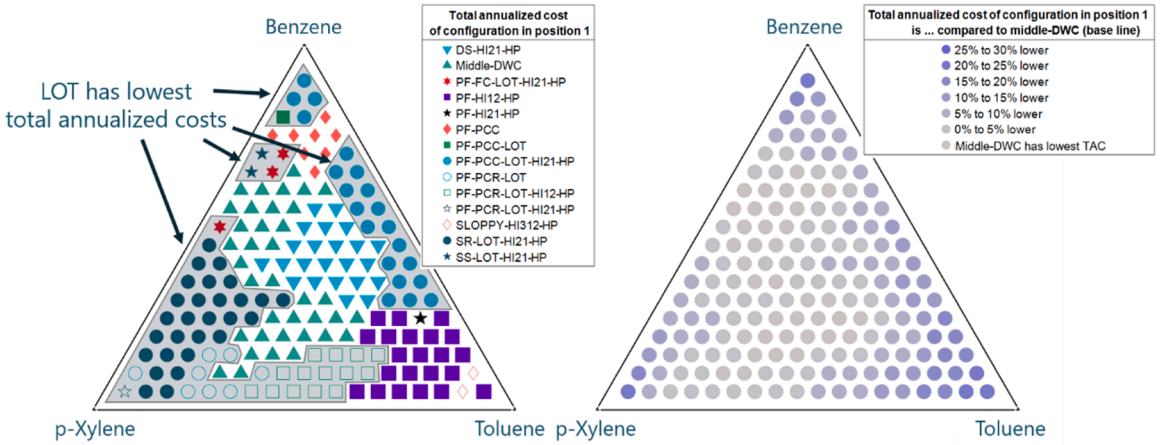

Fig. 17. Best configurations regarding total annualized cost (left) and difference compared to middle-DWC (right) for separation of different feed compositions, excluding configurations with vacuum operation. We refer to the nomenclature at the beginning of this work for interpretation of the configuration identifiers.

Unsurprisingly, without vacuum operation, the relative TAC advantage of heat-integrated configurations over the middle-DWC diminishes and for many compositions, the best-performing above-atmospheric processes achieve TAC savings of less than 10 % compared to the middle-DWC. Yet, for feed compositions rich in a single component, the TAC savings still exceed 20 %, showcasing that significant cost savings can be obtained even when relying solely on above-atmospheric operation. This result underscores the significant economic benefits of LOT-HI configurations, especially in applications where relatively pure feed streams require additional refinement to meet stringent product specifications.

5.3. Rigorous optimization

To verify the savings predicted by the shortcut screening, a rigorous evaluation of seven configurations is performed for a feed rich in heavy boiler (10 mol-% benzene, 10 mol-% toluene, 80 mol-% p-xylene) with all product purities constrained to $\geq$ 99mol %. The direct sequence and middle-DWC serve as benchmark cases, while three LOT-HI configurations with the lowest TAC estimates form the shortcut screening for the selected feed are considered, including two variants of the SR-LOT-HI with pressure reduction and the PF-PCR-LOT-HI12-LP, all of which utilize a single side stream. Additionally, the PF-FC-LOT-HI12-LP as the best configuration with two side streams and the SR-LOT-HI21-HP with the lowest MED and TAC among all non-vacuum processes are considered.

The initial number of stages for each column is assigned based on the number of stages calculated during shortcut screening multiplied with a factor; factors of 1.4 are found typically suitable such that the solution is not at bounds. If the TAC-optimal solution makes use of the maximum number of stages, the number of initial stages is increased such that the solution it is not at bounds.

The sequence of NLPs according to the description in Section 4.2.6 are solved in GAMS 48.4.0 with SNOPT on a PC with an Intel Core i7-13400 CPU. On average, the computation time required for each configuration is only a few minutes. Key design parameters and performance metrics of the techno-economically optimized processes are summarized in Table 1, while Fig. 18 provides a bar graph showing a cost overview for all configurations.

Across all configurations, the rigorous results deviate by less than ±10 % in external energy demand from the shortcut prediction and less than ±5 % in TAC for all sequences not based on the PF. For the prefractionator-based LOT-HI configurations, the TAC deviation of the rigorous results is larger at -16 % (PF-PCR-LOT-HI12-LP) and -22 % (PF-FC-LOT-HI12-LP), indicating these may have larger potential of optimization. Yet, these results confirm that the shortcut screening is a reliable tool for performance estimation of optimal designs.

The larger deviations might result from the fact that both prefractionator-based flowsheets operate the second column at deeper vacuum (0.105 bar) which therefore requires refrigerated water at the condenser operated at ~21 °C, leading to higher cooling costs. In both cases, the feed into the stripping section of the second column is precooled with ordinary cooling water to reduce the need for refrigerated water. A modest pressure increase in both columns (to 1.9 bar and 0.24 bar) could eliminate the need for refrigerated water entirely and unlock additional savings. Interestingly, none of the optimized LOT-HI designs employ feed preheating, such that some solutions use subcooled feed streams, despite the option to avoid this. This likely stems from the influence of the thermal state of the feed on the driving forces for separation, as heating or cooling along the height of the column lowers the driving forces and thus would require more stages.

Fig. 19 provides a more detailed illustration of the optimized process configurations for three of the most economic results, as well as the middle-DWC for further comparison. The middle-DWC reduces external heat by 35 % relative to the direct sequence, but it is also the tallest and widest column, resulting in a capital cost slightly higher than the direct sequence, contrary to the capital savings often reported in the literature. Yet, the energy savings translate to a TAC reduction of 24 % over the direct sequence. However, every LOT-HI variant outperforms both benchmarks on energy and TAC. The PF-FC-LOT-HI12-LP offers the best overall performance with the lowest external heat demand as well the lowest TAC. It requires 70 % less external heat than the direct sequence and 50 % less heat than the middle-DWC translating into TAC-savings of 40 % over the middle-DWC from lower operating and capital costs.

The SR-LOT-HI21-HP is noteworthy because it offers the lowest capital cost of any configuration, still cutting external heat by 26 % and TAC by 11 % relative to the middle-DWC, while avoiding vacuum operation altogether. Its only drawback is the need for more expensive steam in column 2 at a column pressure of 2.65 bar due to the elevated bottom temperature (178.1 °C).

Finally, the comparison between single- and double-side-draw variants shows that multiple process designs achieve similar performance: SR-LOT-HI12-LP and PF-PCR-LOT-HI12-LP with only one side stream achieve TAC values only 3–4 % above the best design. However, while the flowsheet with two side stream appears more complex initially, it offers an additional operational degree of freedom, which may prove beneficial. The molar liquid and vapor flow rates of the PF-FC-LOT-HI12-LP configuration are illustrated in Fig. 20. While the vapor flow rates are relatively constant throughout both columns, the liquid flow increase by a factor of 4 in the first column on the feed stage and drops at stage 34 where the larger side stream is transferred to the second column. This stream also causes a sharp increase in liquid flow rate upon entering stage 23 of the second column, which might require more attention in a detailed equipment design. However, structured packings with proper liquid collectors and redistribution should handle such different liquid loads well without affecting the separation meaningfully. The increased liquid load would increase pressure drop (not modeled) slightly for affected sections [77].

To support the validity of these results on a more general basis, the two sequences with the lowest TAC identified in the shortcut screening as well as the middle-DWC and direct sequence are rigorously optimized for two additional feed compositions where LOT processes are the most economical (90 mol-% benzene, 5 mol-% toluene, 5 mol-% p-xylene and 20 mol-% benzene, 40 mol-% toluene, 40 mol-% p-xylene). The results

Table 1
Key results of TAC-optimal designs for different configurations and shortcut results for comparison (10 mol-% benzene, 10 mol-% toluene, 80 mol-% p-xylene).

Process	Direct sequence	middle-DWC	SR-LOT-HI12-LP	SR-LOT-HI21-LP	SR-LOT-HI21-HP	PF-PCR-LOT-HI12-LP	PF-FC-LOT-HI12-LP
External heat duty (kW)	565.0	369.8	202.7	241.2	273.2	177.6	171.9
External cooling duty (kW)	−551.0	−356.0	−266.4	−264.5	−212.9	−252.0	−234.9
Reflux ratio	4.49 / 10.63	13.92	5.25 / 6.3	4.73 / 5.02	5.96 / 6.33	3.04 / 3.56	6.61 / 11.83
Number of stages	43 / 51	68	54 / 27	43 / 46	55 / 54	30 / 52	56 / 40
Height (m)	23.77 / 27.03	41.06	30.49 / 15.61	23.92 / 24.99	28.39 / 27.97	16.34 / 29.93	31.21 / 22.86
Diameter (m)	0.43 / 0.65	0.72	0.47 / 0.85	0.58 / 0.51	0.49 / 0.46	0.44 / 0.67	0.43 / 0.66
Annual operating cost (k$/a)	234.2	153.3	84.8	100.3	141.4	92.8	88.4
Capital cost (k$)	516.3	580.0	606.0	607.2	486.8	545.6	566.6
Total annual cost (k$/a)	304.4	232.1	167.1	182.8	207.6	169.8	162.5
Computation time (s)	75.6	172.2	117.5	184.2	102.2	398.2	176.0
Shortcut result: External heat duty (kW)	550	387	192	246	278	191	190
Difference: Rigorous external heat duty versus Shortcut results (%)	+2.72	−4.46	+5.60	−1.96	−1.74	−7.00	−9.54
Shortcut result: Total annual cost (k$/a)	296	233	165	189	218	202	208
Difference: Rigorous total annual cost versus Shortcut results (%)	+2.83	−0.41	+1.27	−3.29	−4.79	−15.95	−21.86

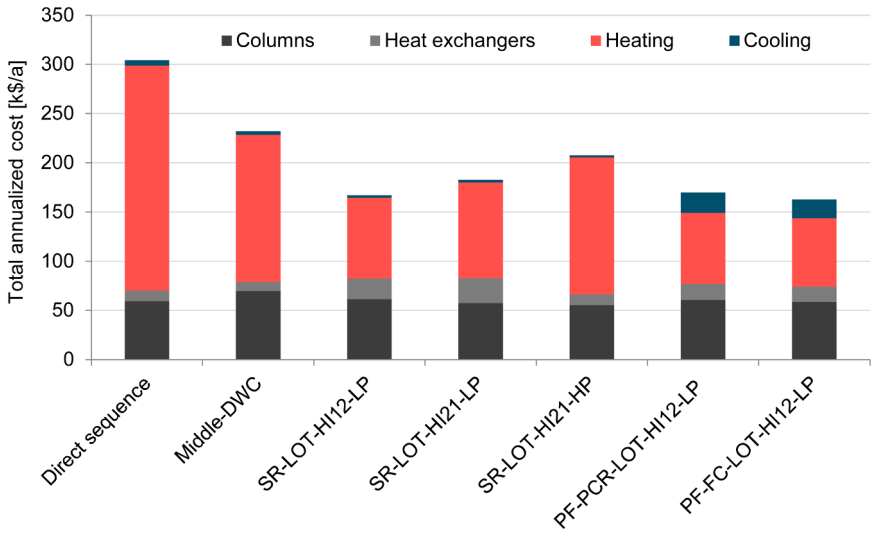

Fig. 18. TAC breakdown of TAC-optimal designs for different configurations (10 mol-% benzene, 10 mol-% toluene, 80 mol-% p-xylene).

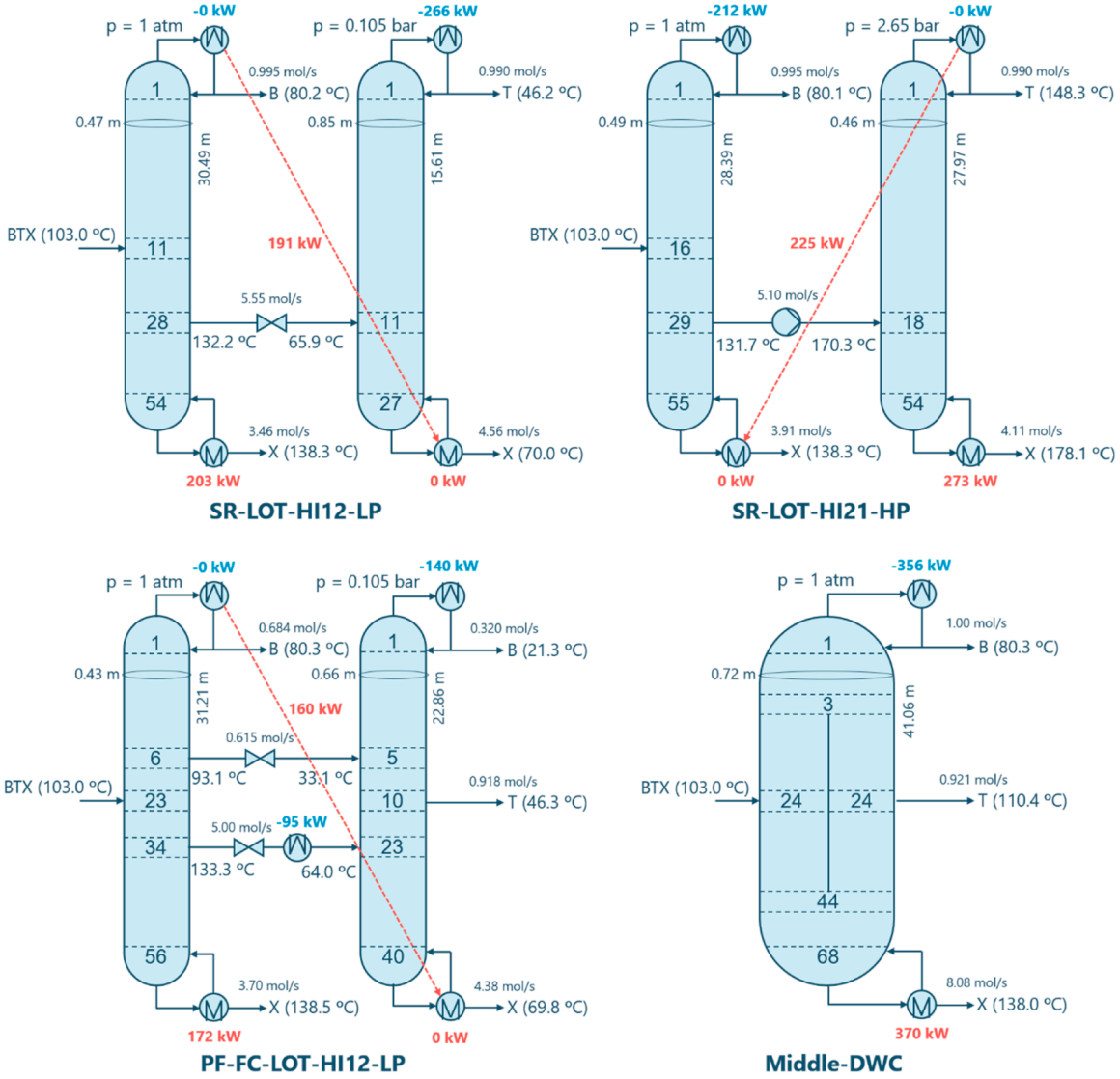

Fig. 19. Flowsheets of TAC-optimal process designs obtained for separating 10 mol-% benzene (B), 10 mol-% toluene (T) and 80 mol-% p-xylene (X).

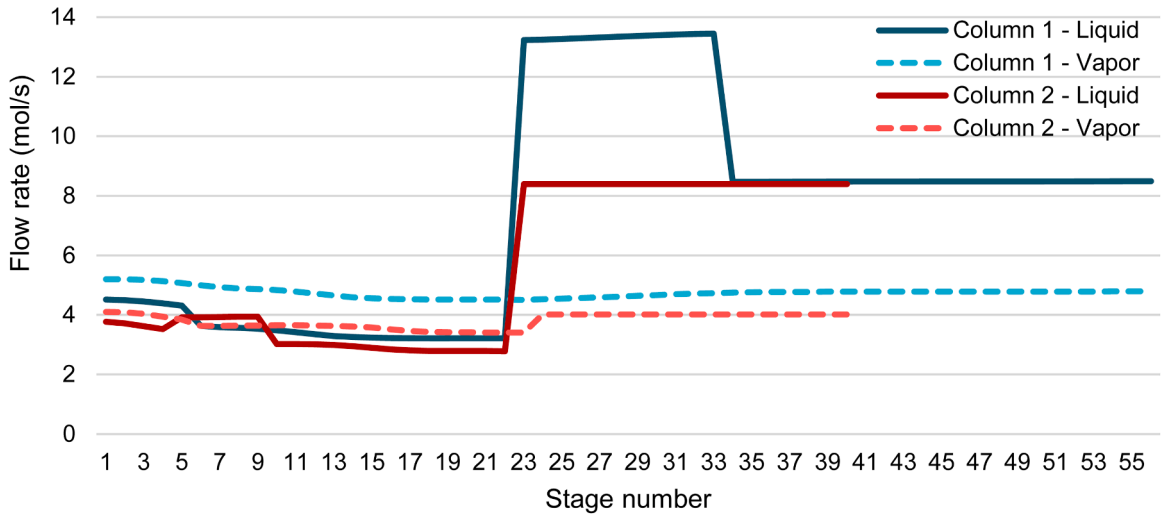

Fig. 20. Liquid and vapor flow rates inside optimal design of PF-FC-LOT-HI12-LP configuration for separation of 10 mol-% benzene, 10 mol-% toluene and 80 mol-% p-xylene.

Table 2
Key results of TAC-optimal designs for two feed compositions and shortcut results for comparison.

Feed composition	90 mol-% benzene, 5 mol-% toluene, 5 mol-% p-xylene				20 mol-% benzene, 40 mol-% toluene, 40 mol-% p-xylene			
Process	Direct sequence	middle-DWC	PF-PCC-LOT-HI21-HP	PF-PCC-LOT	Direct sequence	middle-DWC	PF-PCR-LOT-HI12-LP	PF-HI12-LP
External heat duty (kW)	530.8	410.6	374.4	398.5	650.0	457.7	198.7	246.0
External cooling duty (kW)	−526.1	−406.0	−348.5	−393.9	−635.4	−443.0	−266.8	−333.4
Reflux ratio	0.72 / 1.99	0.62	0.41 / 0.48	0.41 / 0.39	3.03 / 1.92	7.71	0.85 / 2.79	0.94 / 2.58
Number of stages	40 / 44	64	27 / 115	31 / 86	39 / 42	58	49 / 55	21 / 73
Height (m)	22.91 / 23.95	39.69	15.36 / 58.41	16.88 / 44.91	22.34 / 23.61	34.86	26.08 / 28.64	12.98 / 40.48
Diameter (m)	0.71 / 0.23	0.87	0.60 / 0.21	0.60 / 0.23	0.52 / 0.65	0.82	0.46 / 0.74	0.5 / 0.74
Annual operating cost (k$/a)	220.1	170.3	161.8	165.3	269.5	189.7	114.4	135.4
Capital cost (k$)	457.7	676.0	335.8	325.2	513.6	592.6	662.8	706.2
Total annual cost (k$/a)	282.3	262.2	207.5	209.5	339.3	270.2	204.5	231.3
Computation time (s)	44	305	329	280	105	217	232	159
Shortcut result: External heat duty (kW)	528	479	378	428	652	456	220	254
Difference: Rigorous external heat duty versus Shortcut results (%)	+0.53	−14.28	−0.95	−6.89	−0.31	0.37	−9.68	−3.15
Shortcut result: Total annual cost (k$/a)	290	298	226	249	350	269	226	237
Difference: Rigorous total annual cost versus Shortcut results (%)	−2.66	−12.01	−8.19	−15.86	−3.06	+0.45	−9.51	−2.41

of the rigorous optimization are summarized in Table 2 and do again match the shortcut results with a maximum deviation of 16 % for both external energy demand and TAC, while most results show differences between shortcut calculations and rigorous optimization below 10 %. Most importantly the relative ranking of these variants does not change after rigorous optimization, confirming that LOT-HI configurations have the potential for significant savings over the middle-DWC also across different separation tasks. Interestingly, the most economical process for the feed rich in benzene does not even make use of HI, but still provides an almost identical TAC to the best performing LOT-HI configuration. As noted before, the middle-DWC also has higher capital costs than the direct sequence for both other considered feed compositions by up to 48 % for the feed rich in benzene.

6. Conclusion

The primary objective of this work was to determine whether liquid-only-transfer (LOT) side-stream configurations, particularly when combined with direct heat integration (HI), provide a sufficient potential to reduce the net energy requirements and reduce cost compared to other distillation processes, especially the established fully thermally coupled dividing-wall columns. For this purpose, an extension of a previously developed shortcut screening tool with dedicated LOT and LOT-HI configurations was performed together with a dedicated implementation of a rigorous superstructure optimization of such configurations, to validate the most promising results of the shortcut screening on the basis of rigorous MESH models.

The conducted shortcut screening for the separation of a widely investigated benzene, toluene p-xylene case study, revealed that LOT configurations with direct condenser-to-reboiler heat integration can enable significant savings in net energy requirements, as well as total annualized costs, with 15–55 % net energy savings for 171 feed compositions compared to the middle dividing wall column. The LOT-HI configurations provided the minimum net energy demand for 89 % and minimum cost for 46 % of these feed conditions. Especially the heat integrated LOT processes based on the partially coupled prefractionator, which to our knowledge has not received much attention in the existing literature so far, performs extremely well for large range of considered separation tasks.

While the results demonstrate the premise of the process synthesis framework [55] and the high value of a large-scale screening to identify the most promising configurations, the final optimization with rigorous MESH-based superstructure models confirms the results of the shortcut screening and the good accuracy of the approximations. The best LOT-HI

design with two side streams requires 70 % less external heat than the direct sequence and 50 % less than the middle dividing wall column and has the lowest TAC of all configurations for the considered feed composition with high amount of high boiler. Multiple LOT-HI designs offer lower capital cost than the middle dividing wall column, while many top-ranking solutions use only a single side stream, requiring a less complex configuration and a less pronounced temperature lift for heat integration.

Future work on the investigation of the LOT and especially LOT-HI configurations will address some of the considered assumptions. In order to overcome the limitation of the current isobaric models, an incorporation of realistic hydraulics for the rigorous superstructure model can improve the design with better temperature predictions particularly for vacuum operation, for which the process performance may be affected to some considerable degree. Additionally, the different sensible heats of the products can be covered by considering further heat integration to yield equivalent thermal states of the products. Beyond these aspects, further research on operability and controllability of LOT-configurations is needed to investigate the potential offered by the additional degrees of freedom, as emphasized in the review paper of Horsch and Skiborowski [28], as well as experimental investigations to confirm advantages and convince practitioners to employ LOT configurations in industrial settings.

Declaration of generative AI and AI-assisted technologies in the writing process

During the preparation of this work the authors used ChatGPT in order to aid in formulation of text sections. After using this tool/service, the authors reviewed and edited the content as needed and take full responsibility for the content of the publication.

CRediT authorship contribution statement

Momme Adami: Writing – review & editing, Writing – original draft, Visualization, Validation, Software, Project administration, Methodology, Investigation, Data curation, Conceptualization. **Sina Bertram:** Validation, Software, Methodology, Investigation. **Dennis Espert:** Validation, Software, Methodology. **Mirko Skiborowski:** Writing – review & editing, Supervision, Software, Resources, Methodology.

Declaration of competing interest

The authors declare that they have no known competing financial interests or personal relationships that could have appeared to influence the work reported in this paper.

Acknowledgements

This research did not receive any specific grant from funding agencies in the public, commercial, or not-for-profit sectors.

Supplementary materials

Supplementary material associated with this article can be found, in the online version, at doi:10.1016/j.cep.2025.110559.

Data availability

Data will be made available on request.

References

[1] A. Marina, S. Spoelstra, H.A. Zondag, A.K. Wemmers, An estimation of the European industrial heat pump market potential, Renew. Sustain. Energy Rev. 139 (2021) 110545, https://doi.org/10.1016/j.rser.2020.110545.
[2] Enerdata, Carbon Price Forecast Under EU ETS, Executive Brief, 2023.
[3] D.S. Sholl, R.P. Lively, Seven chemical separations to change the world, Nature 532 (7600) (2016) 435–437, https://doi.org/10.1038/532435a.
[4] Oak Ridge National Laboratory, Materials for separation technologies, Energy Emiss. Reduct. Opport. (2005).
[5] R. Agrawal, R.T. Gooty, Misconceptions about efficiency and maturity of distillation, AIChE J. 66 (8) (2020), https://doi.org/10.1002/aic.16294.
[6] E.L. Cussler, B.K. Dutta, On separation efficiency, AIChE J. 58 (12) (2012) 3825–3831, https://doi.org/10.1002/aic.13779.
[7] M. Blahušiak, AA. Kiss, K. Babic, SR.A. Kersten, G. Bargeman, B. Schuur, Insights into the selection and design of fluid separation processes, Sep. Purif. Technol. 194 (2018) 301–318, https://doi.org/10.1016/j.seppur.2017.10.026.
[8] B. Kruber, K. Droste, M. Skiborowski, Thermodynamic efficiency of membrane-assisted distillation processes, AIChE J. (2023), https://doi.org/10.1002/aic.18015.
[9] M. Skiborowski, A. Harwardt, W. Marquardt, Conceptual design of distillation-based hybrid separation processes, Annu. Rev. Chem. Biomol. Eng. 4 (2013) 45–68, https://doi.org/10.1146/annurev-chembioeng-061010-114129.
[10] A.K. Jana, Advances in heat pump assisted distillation column: a review, Energy Convers. Manag. 77 (2014) 287–297, https://doi.org/10.1016/j.enconman.2013.09.055.
[11] A.A. Kiss, F. Landaeta, J. Servando, I. Ferreira, A. Carlos, Towards energy efficient distillation technologies – making the right choice, Energy 47 (1) (2012) 531–542, https://doi.org/10.1016/j.energy.2012.09.038.
[12] M. Adami, J. Schnurr, M. Skiborowski, Electrified distillation – optimized design of closed cycle heat pumps with refrigerant selection and flash-enhanced mechanical vapor recompression, Appl. Therm. Eng. (2025) 126559, https://doi.org/10.1016/j.applthermaleng.2025.126559.
[13] T. Wakabayashi, A. Ferrari, S. Hasebe, Design and commercial operation of a discretely heat-integrated distillation column, Chem. Eng. Res. Des. 147 (2019) 214–221, https://doi.org/10.1016/j.cherd.2019.04.036.
[14] A.A. Shenvi, D.M. Herron, R. Agrawal, Energy efficiency limitations of the conventional heat integrated distillation column (HIDiC) configuration for binary distillation, Ind. Eng. Chem. Res. 50 (1) (2011) 119–130, https://doi.org/10.1021/ie101698f.
[15] M. Adami, K. Farheen, M. Skiborowski, Electrifying distillation – optimization-based evaluation of internally heat-integrated distillation columns, Sep. Purif. Technol. (2024) 131061, https://doi.org/10.1016/j.seppur.2024.131061.
[16] A. Harwardt, W. Marquardt, Heat-integrated distillation columns: vapor recompression or internal heat integration? AIChE J. 58 (12) (2012) 3740–3750, https://doi.org/10.1002/aic.13775.
[17] C. Cui, Z. Xi, S. Liu, J. Sun, An enumeration-based synthesis framework for multi-effect distillation processes, Chem. Eng. Res. Des. 144 (2019) 216–227, https://doi.org/10.1016/j.cherd.2019.02.018.
[18] S. Sabour, S.M. Javad, B. Ghorashi, A comprehensive review of major water desalination techniques and mineral extraction from saline water, Sep. Purif. Technol. 349 (2024) 127913, https://doi.org/10.1016/j.seppur.2024.127913.
[19] Z. Shen, Q. Qu, M. Chen, H. Lyu, J. Sun, Advancements in methanol distillation system: a comprehensive overview, Chem. Eng. Res. Des. 199 (2023) 130–151, https://doi.org/10.1016/j.cherd.2023.09.026.
[20] R. Agrawal, Z.T. Fidkowski, Are thermally coupled distillation columns always thermodynamically more efficient for ternary distillations? Am. Chem. Soc. 37 (1998) 3444–3454.
[21] B. Kaibel, Dividing-Wall columns. Distillation, Elsevier, 2014, pp. 183–199.
[22] G. Lukač, I.J. Halvorsen, Ž. Olujić, I. Dejanović, On controllability of a fully thermally coupled four-product dividing wall column, Chem. Eng. Res. Des. 147 (2019) 367–377, https://doi.org/10.1016/j.cherd.2019.04.041.
[23] A.A. Kiss, Distillation technology - still young and full of breakthrough opportunities, J. Chem. Technol. Biotechnol. 89 (4) (2014) 479–498, https://doi.org/10.1002/jctb.4262.
[24] T. Waltermann, S. Sibbing, M. Skiborowski, Optimization-based design of dividing wall columns with extended and multiple dividing walls for three- and four-product separations, Chem. Eng. Process. - Process Intensif. 146 (2019) 107688, https://doi.org/10.1016/j.cep.2019.107688.
[25] Ž. Olujić, M. Jödecke, A. Shilkin, G. Schuch, B. Kaibel, Equipment improvement trends in distillation, Chem. Eng. Process. - Process Intensif. 48 (6) (2009) 1089–1104, https://doi.org/10.1016/j.cep.2009.03.004.
[26] J.A. Weinfeld, S.J. Owens, R.B. Eldridge, Reactive dividing wall columns: A comprehensive review, Chem. Eng. Process. - Process Intensif. 123 (2018) 20–33, https://doi.org/10.1016/j.cep.2017.10.019.
[27] R. Agrawal, Thermally coupled distillation with reduced number of intercolumn vapor transfers, AIChE J. 46 (11) (2000) 2198–2210, https://doi.org/10.1002/aic.690461112.
[28] A.S. Horsch, M. Skiborowski, Thermally coupled distillation columns without vapor transfer – current state and further needs, Sep. Purif. Technol. 354 (2025) 128762, https://doi.org/10.1016/j.seppur.2024.128762.
[29] Skiborowski, M. (2020): Energy efficient distillation by combination of thermal coupling and heat integration 48, pp. 991–996. DOI: 10.1016/B978-0-12-823377-1.50166-X.
[30] M. Adami, A.S. Horsch, M. Skiborowski, Can simple side stream configurations compete with fully thermally coupled dividing wall columns? Distill. Absorp. 2022 (2022).
[31] K. Kraemer, S. Kossack, W. Marquardt, Efficient optimization-based design of distillation processes for homogeneous azeotropic mixtures, Ind. Eng. Chem. Res. 48 (14) (2009) 6749–6764, https://doi.org/10.1021/ie900143e.

[32] IJ. Halvorsen, S. Skogestad, Minimum energy consumption in multicomponent distillation. 1. Vmin diagram for a two-product column, Ind. Eng. Chem. Res. 42 (3) (2003) 596–604, https://doi.org/10.1021/ie010863g.
[33] IJ. Halvorsen, S. Skogestad, Minimum energy consumption in multicomponent distillation. 2. Three-product petlyuk arrangements, Ind. Eng. Chem. Res. 42 (3) (2003) 605–615, https://doi.org/10.1021/ie0108649.
[34] IJ. Halvorsen, S. Skogestad, Minimum energy consumption in multicomponent distillation. 3. More than three products and generalized Petlyuk arrangements, Ind. Eng. Chem. Res. 42 (3) (2003) 616–629, https://doi.org/10.1021/ie0108651.
[35] G. Kaibel, E. Blass, J. Köhler, Thermodynamics — Guideline for the development of distillation column arrangements, Gas Separ. Purif. 4 (2) (1990) 109–114, https://doi.org/10.1016/0950-4214(90)80037-L.
[36] D. Dwivedi, J.P. Strandberg, I.J. Halvorsen, H.A. Preisig, S. Skogestad, Active vapor split control for dividing-wall columns, Ind. Eng. Chem. Res. 51 (46) (2012) 15176–15183, https://doi.org/10.1021/ie3014346.
[37] G.R. Harvianto, K.H. Kim, K.J. Kang, M. Lee, Optimal operation of a dividing wall column using an enhanced active vapor distributor, Chem. Eng. Res. Des. 144 (2019) 512–519, https://doi.org/10.1016/j.cherd.2019.02.038.
[38] K.J. Kang, G.R. Harvianto, M. Lee, Hydraulic driven active vapor distributor for enhancing operability of a dividing wall column, Ind. Eng. Chem. Res. 56 (22) (2017) 6493–6498, https://doi.org/10.1021/acs.iecr.7b01023.
[39] D. Staak, T. Grützner, B. Schwegler, D. Roederer, Dividing wall column for industrial multi purpose use, Chem. Eng. Process. - Process Intensif. 75 (2014) 48–57, https://doi.org/10.1016/j.cep.2013.10.007.
[40] L.-M. Ränger, I.J. Halvorsen, T. Grützner, S. Skogestad, What can go wrong in a dividing wall column and how to detect it, Sep. Purif. Technol. 354 (2025) 129151, https://doi.org/10.1016/j.seppur.2024.129151.
[41] I. Dejanović, L. Matijašević, I.J. Halvorsen, S. Skogestad, H. Jansen, B. Kaibel, Ž. Olujić, Designing four-product dividing wall columns for separation of a multicomponent aromatics mixture, Chem. Eng. Res. Des. 89 (8) (2011) 1155–1167, https://doi.org/10.1016/j.cherd.2011.01.016.
[42] S. Jia, X. Qian, X. Yuan, Optimal design for dividing wall column using support vector machine and particle swarm optimization, Chem. Eng. Res. Des. 125 (2017) 422–432, https://doi.org/10.1016/j.cherd.2017.07.028.
[43] T. Waltermann, M. Skiborowski, Conceptual design of highly integrated processes - optimization of dividing wall columns, Chemie Ingenieur Technik 89 (5) (2017) 562–581, https://doi.org/10.1002/cite.201600128.
[44] R.R. Rewagad, A.A. Kiss, Dynamic optimization of a dividing-wall column using model predictive control, Chem. Eng. Sci. 68 (1) (2012) 132–142, https://doi.org/10.1016/j.ces.2011.09.022.
[45] R.C. van Diggelen, A.A. Kiss, A.W. Heemink, Comparison of control strategies for dividing-wall columns, Ind. Eng. Chem. Res. 49 (1) (2010) 288–307, https://doi.org/10.1021/ie9010673.
[46] I. Dejanović, I.J. Halvorsen, S. Skogestad, H. Jansen, Ž. Olujić, Hydraulic design, technical challenges and comparison of alternative configurations of a four-product dividing wall column, Chem. Eng. Process. - Process Intensif. 84 (2014) 71–81, https://doi.org/10.1016/j.cep.2014.03.009.
[47] U. Preißinger, G. Lukač, I. Dejanović, T. Grützner, Investigation of control structures for a four-product laboratory multiple dividing-wall column using dynamic simulation, Chem. Eng. Technol. 44 (2) (2021) 223–237, https://doi.org/10.1002/ceat.202000557.
[48] Y. Waibel, L. Trescher, L.-M. Ränger, T. Grützner, First multiple dividing wall column: design and operation, Chem. Eng. Res. Des. 193 (2023) 132–144, https://doi.org/10.1016/j.cherd.2023.03.017.
[49] Yi Zheng, Z. Wang, H. Pan, H. Ling, Initial design and multi-objective optimization of four-product dividing wall column, Sep. Purif. Technol. 309 (2023) 122961, https://doi.org/10.1016/j.seppur.2022.122961.
[50] R. Agrawal, Multieffect distillation for thermally coupled configurations, AIChE J. 46 (11) (2000) 2211–2224, https://doi.org/10.1002/aic.690461113.
[51] R. Agrawal, Z.T. Fidkowski, Improved direct and indirect systems of columns for ternary distillation, AIChE J 44 (4) (1998) 823–830.
[52] A.S. Horsch, A.R. Acevedo, M. Skiborowski, Optimal retrofit of simple distillation sequences to thermally coupled side-stream configurations, in: 33rd European Symposium on Computer Aided Process Engineering 52, Elsevier, 2023, pp. 331–336 (Computer Aided Chemical Engineering).
[53] G.M. Ramapriya, M. Tawarmalani, R. Agrawal, Thermal coupling links to liquid-only transfer streams: an enumeration method for new FTC dividing wall columns, AIChE J. 62 (4) (2016) 1200–1211, https://doi.org/10.1002/aic.15053.
[54] IJ. Halvorsen, S. Skogestad, Liquid-only transfer in dividing wall columns – Analytical minimum vapor expressions, Sep. Purif. Technol. 365 (2025) 132530, https://doi.org/10.1016/j.seppur.2025.132530.
[55] W. Marquardt, S. Kossack, K. Kraemer, A framework for the systematic design of hybrid separation processes, Chin. J. Chem. Eng. 16 (3) (2008) 333–342, https://doi.org/10.1016/S1004-9541(08)60084-1.
[56] M. Skiborowski, Fast screening of energy and cost efficient intensified distillation processes, Chem. Eng. Trans. 69 (2018) 199–204, https://doi.org/10.3303/CET1869034.
[57] M. Adami, D. Espert, M. Skiborowski, Pimp my distillation sequence shortcut-based screening of intensified configurations, in: Proceedings of the 35th European Symposium on Computer Aided Process Engineering (ESCAPE 35). The 35th European Symposium on Computer Aided Process Engineering, PSE PressHamilton, Canada (Systems and Control Transactions), Ghent, Belgium, 2025, pp. 2630–2636, 06.07.2025 - 09.07.2025.
[58] M. Adami, D. Espert, M. Skiborowski, Rapid multi-criteria screening of energy-integrated distillation processes for nonideal mixtures, Sep. Purif. Technol. (2025) 134463, https://doi.org/10.1016/j.seppur.2025.134463.
[59] M. Skiborowski, A. Harwardt, W. Marquardt, Efficient optimization-based design for the separation of heterogeneous azeotropic mixtures, Comput. Chem. Eng. 72 (5) (2015) 34–51, https://doi.org/10.1016/j.compchemeng.2014.03.012.
[60] J. Bausa, R.v. Watzdorf, W. Marquardt, Minimum energy demand for nonideal multicomponent distillations in complex columns, Comput. Chem. Eng. 20 (1996) S55–S60, https://doi.org/10.1016/0098-1354(96)00020-8.
[61] J. Bausa, R. von Watzdorf, W. Marquardt, Shortcut methods for nonideal multicomponent distillation: I. Simple columns, AIChE J. 44 (10) (1998) 2181–2198, https://doi.org/10.1002/aic.690441008.
[62] R. von Watzdorf, J. Bausa, W. Marquard, Shortcut methods for nonideal multicomponent distillation: 2. Complex columns, AIChE J. 45 (8) (1999) 1615–1628.
[63] AVT.SVT at RWTH Aachen University, Process Synthesis Softwarecollection, Process Anal. Des. Routines (2014). Available online at, https://www.avt.rwth-aachen.de/cms/avt/forschung/sonstiges/software/~iptu/softwaresammlung-prozesssynthese/?lidx=1. checked on 2/10/2025.
[64] F.W. Winn, New relative volatility method for distillation calculations, Petrol. Refin. 37 (5) (1958) 216–218.
[65] J.M. Douglas, Conceptual Design of Chemical Processes, McGraw-Hill Publishing Company (McGraw-Hill chemical engineering series), New York, 1988.
[66] R. Turton, R.C. Bailie, W.B. Whiting, J.A. Shaeiwitz, Analysis, synthesis, and Design of Chemical Processes, 3rd ed., Pearson Education, Upper Saddle River, New Jersey, 2009 [distributor] (Prentice Hall PTR international series in the physical and chemical engineering sciences).
[67] LT. Biegler, IE. Grossmann, AW. Westerberg, Systematic Methods of Chemical Process Design, Prentice Hall PTR (Prentice Hall PTR international series in the physical and chemical engineering sciences), Upper Saddle River, New Jersey, 1997.
[68] M.A. Navarro, J. Javaloyes, J.A. Caballero, I.E. Grossmann, Strategies for the robust simulation of thermally coupled distillation sequences, Comput. Chem. Eng. 36 (2012) 149–159, https://doi.org/10.1016/j.compchemeng.2011.06.014.
[69] T. Waltermann, M. Skiborowski, Efficient optimization-based design of energy-integrated distillation processes, Comput. Chem. Eng. 129 (8) (2019) 106520, https://doi.org/10.1016/j.compchemeng.2019.106520.
[70] J. Kallrath, Polylithic modeling and solution approaches using algebraic modeling systems, Optim. Lett. 5 (3) (2011) 453–466, https://doi.org/10.1007/s11590-011-0320-4.
[71] C. Cui, Q. Zhang, X. Zhang, J. Sun, Eliminating the vapor split in dividing wall columns through controllable double liquid-only side-stream distillation configuration, Sep. Purif. Technol. 242 (2020) 1–15, https://doi.org/10.1016/j.seppur.2020.116837.
[72] C. Cui, X. Zhang, J. Sun, Design and optimization of energy-efficient liquid-only side-stream distillation configurations using a stochastic algorithm, Chem. Eng. Res. Des. 145 (2019) 48–52, https://doi.org/10.1016/j.cherd.2019.03.001.
[73] M.M. Donahue, B.J. Roach, J.J. Downs, T. Blevins, M. Baldea, R.B. Eldridge, Dividing wall column control: common practices and key findings, Chem. Eng. Process. - Process Intensif. 107 (2016) 106–115, https://doi.org/10.1016/j.cep.2016.05.013.
[74] Y.H. Kim, Energy savings in the benzene-toluene-xylene separation process using an extended divided-wall column, Chem. Eng. Technol. 39 (12) (2016) 2312–2322, https://doi.org/10.1002/ceat.201500605.
[75] F. Duanmu, E. Sorensen, Optimal design of reduced vapor transfer dividing wall structures with and without heat integration, AIChE J. 70 (11) (2024), https://doi.org/10.1002/aic.18572. Article e18572.
[76] S. Brüggemann, W. Marquardt, Rapid screening of design alternatives for nonideal multiproduct distillation processes, Comput. Chem. Eng. 29 (1) (2004) 165–179, https://doi.org/10.1016/j.compchemeng.2004.07.009.
[77] L. Spiegel, M. Duss, Structured packings, in: A. Górak, Z. Olujic (Eds.), Distillation: Equipment and Processes, Elsevier, 2014, pp. 145–181.